A model study on changes of European and Swiss particulate matter, ozone and nitrogen deposition between 1990 and 2020 due to the revised Gothenburg protocol

S. Aksoyoglu, J. Keller, G. Ciarelli, A. S. H. Prévôt and U. Baltensperger

Laboratory of Atmospheric Chemistry, Paul Scherrer Institute, CH-5232 Villigen PSI

Correspondence to : S. Aksoyoglu (sebnem.aksoyoglu@psi.ch)

Abstract

We report a study of changes in air quality due to emission reductions using the chemical transport model CAMx. The model domain includes all of Europe with a nested domain over Switzerland. The model simulations were performed with emissions for 1990 (the reference year for the Gothenburg Protocol), 2005 (the reference year for the revised Gothenburg Protocol), 2006 (for model validation) and 2020 (the target year for the revised Gothenburg Protocol) using three emission scenarios prepared by IIASA/GAINS. Changes in ozone, particulate matter, and nitrogen deposition are the central theme of the study.

The modelled relative changes in the annual average $PM_{2.5}$ concentrations between 1990 and 2005 look reasonable based on various PM10 and PM2.5 observations in the past. The results obtained in this study suggest that annual mean concentrations of $PM_{2.5}$ decreased by about 20 – 50% in Europe. Simulations using the baseline scenario (BL 2020) suggest that $PM_{2.5}$ concentrations in 2020 will be about 30% lower than those in 2005. The largest predicted decrease in $PM_{2.5}$, based on the MTFR (Maximum Technically Feasible Reduction) scenario, was about 60% and was located mainly in the eastern part of Europe.

In the case of ozone, both model results and measurements show an increase in the mean ozone mixing ratios between 1990 and 2005. The observations, however, suggest a larger increase, indicating the importance of background ozone levels. Although emission reductions caused a decrease in peak ozone values, average ozone levels in polluted regions increased due to reduced titration with nitric oxide (NO). This caused a change in the frequency distribution of ozone. Model simulations using emission scenarios for 2020 suggest that annual average ozone mixing ratios will continue to increase. Changes in the levels of the damage indicators AOT40 for forests and SOMO35 are reported as well.

The model results suggest that nitrogen deposition decreased by 10 - 30% in the eastern part of Europe since 1990, while it increased by about 20% in the Iberian Peninsula. The decrease is mainly due to the deposition of oxidized nitrogen species, whereas deposition of reduced nitrogen compounds increased. In Switzerland, nitrogen deposition is larger in the northern part of the Alps where ammonia emissions are the highest. Applying the baseline scenario, we found that the deposition of oxidized nitrogen compounds will have decreased by a further 40% by 2020, whereas deposition of reduced species will continue to increase. This will lead to a 10 - 20% decrease in the total nitrogen deposition in most of the model domain, with a 10% increase in the eastern part of Europe.

1 Introduction

One of Europe's main environmental concerns is air pollution. Current policy in this respect focuses mainly on ozone (O_3) and particulate matter (PM_{10} and $PM_{2.5}$, particles smaller than 10 and 2.5 μm in aerodynamic diameter, respectively). The policies were especially successful for particulate matter with substantial decreases in the past (Barmpadimos et al., 2012) whereas observed annual mean ozone concentrations did not significantly change (Wilson et al., 2012). Ozone and in spite of the improvements also PM_{10} levels often exceed the ambient air quality standards in Europe, which are: 120 $\mu g\ m^{-3}$ maximum daily 8-hour mean for O_3 and 50 $\mu g\ m^{-3}$ daily mean for PM_{10} (Engler et al., 2012; Hettelingh et al., 2013).

In an earlier study, we reported the effects of numerous regulations enforced in Europe since 1985 and predicted the effects of the Gothenburg protocol targets for 2010 on ozone (Andreani-Aksoyoglu et al., 2008). Our results suggested that the decrease in local ozone production due to emission reductions was partly or completely offset by a simultaneous increase in the background ozone, indicating that further development of background ozone concentrations in Europe would be very important for tropospheric ozone levels. The concentration of ozone in Europe is affected by emissions from other continents due to its long atmospheric lifetime. While ozone precursor emissions in Europe and in North America have decreased significantly since the 1980s, NO_x (NO and NO_2) emissions have increased dramatically in Asia in the last decade (Zhang et al., 2010). Also changes of the flux of stratospheric ozone may be important (Ordonez et al., 2007).

The major indicators used to characterize ozone damage are AOT40 (Accumulated dose of ozone Over the Threshold of 40 ppb) and SOMO35 (Sum of Ozone Means Over 35 ppb). AOT40 is an indicator of damage to vegetation (Ashmore and Wilson, 1992). The UNECE has set the critical level for forest damage at 10000 µg m^{-3} h. SOMO35, on the other hand, was recommended by WHO to be used for health impact assessment (Amann et al., 2008). It is defined as the yearly sum of the daily maximum of 8-hour running average over 35 ppb. It is expected that the strong efforts that have been made to reduce ozone precursor emissions in Europe should decrease the levels of both of these indicators.

In 2007, the Convention on Long-Range Transboundary Air Pollution initiated the revision of its Gothenburg multi-pollutant/multi-effect protocol (UNECE, 1999). Fine particulate matter ($PM_{2.5}$) was included in the revised protocol for which the target year is 2020. In the same context, the EMEP Centre for Integrated Assessment Modelling (CIAM) at IIASA prepared various emission control scenarios for cost-effective improvements to air quality in Europe in 2020 using the GAINS (Greenhouse gas – Air pollution Interactions and Synergies) model.

These developments provided the motivation for this study, in which we used the CAMx air quality model to investigate the changes in European and Swiss air quality between 1990 and 2005 and to predict the effects of various emission reduction scenarios on air quality in 2020 in Europe and in Switzerland. In this paper, we discuss the changes in annual average concentrations of particulate matter, ozone, ozone damage indicators AOT40 and SOMO35 as well as changes in nitrogen deposition between 1990 and 2020.

2 Method

2.1 Model setup

The models used in this study are the Comprehensive Air quality Model with extensions, CAMx, Version 5.40 (http://www.camx.com) and the Weather Research & Forecasting Model (WRF-ARW), Version 3.2.1 (http://wrf-model.org/index.php). The coarse model domain covered all of Europe with a horizontal resolution of 0.250º x 0.125º. A second, nested domain with three times higher resolution (0.083º x 0.0417º) covered Switzerland. The meteorological fields were calculated for 2006 and used for all emission scenarios (see Table 1). We used 6-hour ECMWF data (http://www.ecmwf.int/) to provide initial and boundary conditions for the WRF model. There were 31 terrain-following σ- layers up to 100 hPa in WRF, of which 14 were used in CAMx. The lowest CAMx layer was 20 m above ground and the model top corresponded to about 7000 m above sea level. The initial and boundary concentrations for the coarse domain were

obtained from the MOZART global model data for 2006 (Horowitz et al., 2003). The boundary conditions were kept constant for all future emission scenarios. The choice of background ozone is crucial for air quality simulations and for predicting the effect of emission reductions (Andreani-Aksoyoglu et al., 2008). A recent analysis of various ozone observational data in Europe showed that annual mean ozone concentration increased in the 1980s and 1990s (Logan et al., 2012). Summer ozone levels started decreasing slowly in the 2000s, but there were no significant changes in other seasons. Logan et al. (2012) indicated the inconsistencies in various data sets leading to different trends. It is therefore difficult to choose a realistic background ozone values for the model domain and for the period of interest. In view of this, we kept the background ozone levels constant for simulations in the period between 2005 and 2020 (Wilson et al., 2012; Logan et al., 2012). For the 1990 simulation, background ozone mixing ratios were set about 5 ppb lower in each model layer for all boundaries and for each hour, based on the positive trend in the 1990s reported by the long-term measurement studies (Cui et al., 2011, Logan et al., 2012). Seasonal variation was also taken into account. Photolysis rates were calculated using the TUV photolysis pre-processor (Madronich, 2002). The required ozone column densities were extracted from TOMS data (NASA/GSFC, 2005). Dry deposition of gases in CAMx is based on the resistance model of Zhang et al. (2003). For surface deposition of particles, CAMx includes diffusion, impaction and/or gravitational settling. CAMx uses separate scavenging models for gases and aerosols to calculate wet deposition. The gas-phase mechanism used in this study was CB05 (Carbon Bond Mechanism 5) (Yarwood et al., 2005).

We performed CAMx simulations for 1990 (the reference year for the Gothenburg Protocol), 2005 (the reference year for the revised Gothenburg Protocol), 2006 (for model validation) and 2020 (the target year for the revised Gothenburg Protocol) with different emission scenarios as described in the next section. For all of these simulations, however, the 2006 meteorology was used.

In order to determine the changes in pollutant concentrations in the past (since 1990) and in the future (until 2020), the annual average ozone and $PM_{2.5}$ for each scenario were compared with those in the reference year 2005. Dry and wet deposition of nitrogen species were summed over the entire year for each scenario and compared with 2005. AOT40 for forests was calculated for the daytime hours (8:00 AM – 8:00 PM) from the beginning of April until the end of September in all scenarios. SOMO35 was calculated by summing the daily maximum of the 8-hour running average over 35 ppb for the whole year.

2.2 Emissions

We prepared six emission scenarios (see Table 1). The gridded (0.125º x 0.0625º) TNO/MACC data (http://www.gmes-atmosphere.eu/) for 2006 were used as the basic anthropogenic emission inventory (Denier van der Gon et al., 2010). The European values in both domains were replaced by the high-resolution Swiss emission data for grid cells located within the Swiss national boundary (INFRAS, 2010; Heldstab and Wuethrich, 2006; Kropf, 2001; Heldstab et al., 2003; Schneider, 2007; Kupper et al., 2010). The output of the CAMx simulation using the meteorological data and emissions for 2006 was used for model evaluation.

The TNO/MACC emission inventory was scaled with the annual data from The Centre for Emission Inventories and Projections (CEIP) of the European Monitoring and Evaluation Programme (EMEP), and The International Institute for Applied Systems Analysis/Greenhouse Gas and Air Pollution Interactions and Synergies Model (IIASA/GAINS) was used to prepare gridded, hourly emissions for 1990, 2005 and 2020.

CEIP manages a database of annual emissions before 2009 based on data submitted by participating countries (http://www.ceip.at/webdab-emission-database/emissions-as-used-in-emep-models/). IIASA uses the GAINS model to predict national emission projections until 2020 on the basis of the assumed economic development of each country (http://gains.iiasa.ac.at/gains/EUN/index.login). The emissions for a given emission scenario were calculated by scaling the raw data using annual emission totals for each country, species and SNAP (Selected Nomenclature for Air Pollution) category. For scenarios 1990 and 2005, the annual emissions for each SNAP category were extracted from the EMEP/CEIP database, which contains the historic emissions submitted by the EMEP member states. Data for $PM_{2.5}$ and PM_{10} are only available for 2000 and later, so the 1990 data were calculated from the 2005 data, using GAINS simulations. For the 2020 scenarios, the 2005 data were scaled to 2020 using GAINS CIAM4 / 2011 simulations. The baseline scenario (BL) assumes that emissions will continue to be regulated by the current legislation. The MTFR (maximum technically feasible reductions) scenario uses the lowest expected emissions for most of the source categories. The MID scenario uses moderate emission reductions that are between those of BL and MTFR.

The relative changes in emissions between 2005 and 2020 for various scenarios in Switzerland (CH) and an average of 27 European countries (EU) are shown in Fig. 1. The emissions for the revised Gothenburg Protocol (2020 rev) are included in the figure, although there was no GAINS scenario available at the time of this work. After its publication, however, the reductions specified by the revised Gothenburg Protocol were found to be very close to those for the baseline (2020 BL). In general, emission reductions increase with increasing ambition, i.e. they are lowest in BL and highest in MTFR. The relative changes for Switzerland are usually lower than those for the EU countries (due to the larger emission reductions that had previously been imposed in Switzerland) except for $PM_{2.5}$ for which all reductions are comparable.

The biogenic emissions were calculated using the method described in Andreani-Aksoyoglu and Keller (1995) for each CAMx domain using the temperature and shortwave irradiance from the WRF output, the global USGS land use data and the GlobCover 2006 inventory. For each European country the deciduous and coniferous forest fractions were split into tree species according to the method reported in Simpson et al. (1999). Inside the Swiss border the global data were replaced by data based on land use statistics (100 m resolution) and by forest data (1 km resolution) taken from the national forest inventory (Mahrer and Vollenweider, 1983). Currently this biogenic emission inventory is being improved by extending the number of species and trees, using the best available land use data and including updated temperature and irradiance dependencies (Oderbolz et al., 2013).

3 Results and discussion

3.1 Model evaluation

The results from the lowest layer of both model domains were compared with various observations in 2006. The comparison of modelled meteorological parameters with observations is given in Fig. S1 of the Supplement. In general the agreement between measurements and model results was good with high correlation coefficients (0.76-0.98) and low mean bias error, MBE (0.00023 for specific humidity, -1.13 for air temperature, 0.57 for wind speed). These values fulfil the desired accuracy suggested by Cox et al. (1998) which is 2 ^{o}C for temperature, 1 m s^{-1} and 2.5 m s^{-1} for wind speeds < 10 m s^{-1} and > 10 m s^{-1}, respectively.

The predicted concentrations of ozone and $PM_{2.5}$ in the European domain were compared with measurements at the rural background stations of the European Air quality database AirBase (http://acm.eionet.europa.eu/databases/airbase/). Table 2 gives the overall statistical parameters for all of the year 2006 (only those stations below 500 m asl and with 80% of data available were used for the statistical analysis and these sites cover a large part of Europe between -8.8 and 27.7 degrees from west to east, and between 37.3 and 60.5 from south to north). Mean annual O_3 and $PM_{2.5}$ are slightly over-and under-estimated, respectively. In the case of ozone, although the temporal variation is captured, the maximum concentrations in summer are underestimated as reported by other studies (Fig. 2, upper panel). For instance, evaluation of several air quality models for 2006 within the Air Quality Model Evaluation International Initiative (AQMEII) showed that the models have a predominant tendency to underestimate (in some cases significantly) the peak daily mixing ratio in summertime as well as to overestimate night time mixing ratios with the exception of central Europe (Solazzo et al., 2012a). Time series show that the model reproduced the temporal variation of $PM_{2.5}$ quite well, except for January-February when unusually high concentrations were recorded in Europe (Fig. 2, lower panel). The underestimation of $PM_{2.5}$ is partly due to the severe meteorological conditions prevailing during that exceptionally cold inversion period. It is also possible, however, that the contribution of wood burning to emissions was underestimated. As reported by Solazzo et al (2012b) none of the models used in AQMEII study consistently matched PM2.5 observations for all locations throughout the entire year. Results of the AQMEII study suggest that while the models do relatively well in simulating the inorganic aerosol species, large uncertainty remains in the simulation of other components such as secondary organic aerosols and unspeciated PM2.5. Elimination of the sources of PM bias in the models is still challenging.

The frequency distributions of modelled and measured ozone and PM_{10} values in 2006 are shown in Fig. 3. Comparison of the model results from the nested domain with measurements in Switzerland suggests that the model performance is better at rural sites. At the rural site, Chaumont, for example, the shape of the measured and modelled distributions of O_3 is similar: both have the highest number of points approximately in the middle of the graph. At the urban site, Zurich, on the other hand, the discrepancy between the measurements and model results at low concentrations are clearly seen. Because of the finite model resolution, NO_x concentrations are usually underestimated at urban sites, where local emissions are relatively high and variable. This leads to overestimation of ozone at night and in the morning. In addition to the model horizontal resolution, its representation of the inversion layer at night and the mixing layer during the day also plays an important role in the prediction of pollutant concentrations. In the case of PM_{10}, the measured and modelled concentrations also show a very similar distribution at the rural site Chaumont, indicating very good model performance, whereas the high concentrations at the urban background site, Zurich, were underestimated.

The modelled concentrations of particulate species in the nested domain were compared with AMS (Aerosol Mass Spectrometer) measurements of particulate nitrate, sulphate, ammonium, and organic aerosols (Lanz et al., 2010) in June 2006 at Payerne (Fig. 4). Although the model calculates $PM_{2.5}$ and the AMS measures only particles smaller than 1 μm, the results may be compared, because the difference between PM_1 and $PM_{2.5}$ measurements is very small as shown in Aksoyoglu et al. (2011). Elemental carbon (EC) data are obtained from Aethalometer equivalent black carbon (BC) measurements. The model performance for aerosol components in this study is significantly better than that in our previous study, which used the MM5 meteorological model with an earlier CAMx version (Aksoyoglu et al., 2011). The modelling of organic

aerosols, however, is still quite challenging, mainly due to limited knowledge about the processes involved in secondary organic aerosol (SOA) formation. The CAMx model used in this study includes an SOA model based on a theory of the gas-particle partitioning of various precursors, such as anthropogenic and biogenic VOC species. The oligomerization process, which leads to an increase in aerosol concentrations, is also included. The model performance for organic aerosols is reasonably good for relatively low concentrations. It becomes worse, however, when the formation of secondary organic aerosols increases. The total modelled $PM_{2.5}$ (sum of inorganic and organic species) concentrations match the observations quite well, with one exception on 14-16 June, which was due to underestimation of increased levels of organic aerosols. Models that take into account the volatility distribution and atmospheric aging of OA might give more realistic results (Bergström et al., 2012).

3.2 Particulate matter

The modelled annual average $PM_{2.5}$ concentrations vary between 5 and 40 $\mu g\ m^{-3}$ for the reference year 2005 in Europe (Fig. S2 of the Supplement). Our results suggest that $PM_{2.5}$ concentrations decreased significantly in Europe between 1990 and 2005. The relative changes range from -20% in Scandinavia to more than -60% in the eastern part of the domain; they are between -40 and -45% in central Europe (Fig. 5). There have been long-term measurements of PM_{10} throughout Europe since the late nineties, but measurements of $PM_{2.5}$ at some European sites are available only after 2000 (Tørseth et al., 2012). The available data, however, show average changes between 2000 and 2009 of -18% and -27% for PM_{10} and $PM_{2.5}$, respectively. Recently Cusack et al. (2012) reported that $PM_{2.5}$ concentrations in various parts of Europe decreased by 7-49% between 2002 and 2010. The average trends of $-0.4\ \mu g\ m^{-3}\ y^{-1}$ for PM_{10} and $PM_{2.5}$ at several European sites reported by Barmpadimos et al. (2012) correspond to a decrease of about 40-45% between 1998 and 2010. The PM_{10} measurements at various sites in Switzerland indicate a large decrease (20-56%) between 1991 and 2008 (Barmpadimos et al., 2011). This supports our model results (see Fig. 5), because most of the change in PM_{10} was in the $PM_{2.5}$ fraction (Barmpadimos et al., 2012). Combining the PM10 trends from Barmpadimos et al. (2011) with the modelled PM10 for 1990, 2005 and 2006 in this study at four stations shows the interannual variability in the observed trends together with the emission-induced changes modelled in this study (Fig. S3 of the Supplement).

Changes in particulate matter concentrations result not only from changes in primary PM emissions, but also from changes in precursor emissions such as nitrogen oxides (NO_x), non-methane volatile organic compounds (NMVOC), sulphur dioxide (SO_2) and ammonia (NH_3). As seen in Fig. 1, the European emission reduction of NH_3 for the 2020 scenarios is much smaller than the reduction of other precursor emissions. We compared the predicted annual mean $PM_{2.5}$ concentration for 2020 with that of the reference year (2005) and found that a considerable reduction in $PM_{2.5}$ would be obtained in Europe under the BL scenario (Fig. 6). The decrease in $PM_{2.5}$ would vary from 30-40% in central Europe, up to 50% at some local polluted areas in Eastern Europe. The predicted reductions using the MID and MTFR scenarios are about 50-60%, with the largest changes being predicted in the Balkan countries (only MTFR is shown in the lower panel of Fig. 6.) In Switzerland the predicted reductions in $PM_{2.5}$ are 30 and 40%, using BL and MTFR scenarios, respectively.

3.3 Ozone

The average ozone mixing ratios for the reference year (2005) are shown in Fig. S4 of the Supplement. The model results - based on the assumption that the background

ozone levels increased by 5 ppb between 1990 and 2005 - suggest that the average annual ozone increased between 1990 and 2005 in a large part of Europe in spite of the large reductions of precursor emissions (Fig. 7). The increase in ozone was predicted especially for England, the Benelux countries and around Ukraine. In an earlier sensitivity study, we reported that these areas have VOC-limited regimes for ozone production (Aksoyoglu et al., 2012); a reduction of precursor emissions leads to an increase in ozone levels in such regions.

The impact of the choice of boundary conditions for 1990 on the results shown in Fig. 7 was investigated by a sensitivity test in which we increased the background ozone by 5 ppb. The results suggested that the change in the annual mean ozone (Fig. 7) would be 1-2 ppb lower in central Europe. Long-term observations however, show a significant positive trend in the annual mean ozone especially between 1990 and 2000 (Cui et al., 2011, Logan et al., 2012). A positive trend of 0.32 ppb/y reported by Cui et al. (2011) for annual mean ozone measured at Jungfraujoch between 1990 and 2008 supports our choice of 5 ppb increase in the background ozone between 1990 and 2005.

The predicted O_3 increase is about 1-2 ppb (3-9%) over the Swiss Plateau, whereas observations indicate larger changes between 10% at rural areas and 40-50% at urban sites (Table 3). On the other hand, modelled peak ozone values are lower in 2005 than in 1990 (see Table 4). Measurements also show a decrease in peak ozone levels except in Basel (suburban) and Zurich (urban). The simulation of ozone trends is quite challenging, as has been shown in other model studies (Colette et al., 2011; Wilson et al., 2012). As seen in the example for Zurich, the frequency distribution of ozone mixing ratios in 1990 and 2005 is clearly different (Fig. 8). The most frequent ozone levels are shifted toward higher levels in 2005 and the change is larger in the measurements.

The relative change in annual average ozone mixing ratios between 2005 and 2020 is shown in Figs. 9a and 9b for the European and Swiss domains, respectively. For both BL and MTFR scenarios, the predicted decrease is small (< 4 ppb, < 10%) in central Europe, whereas ozone is expected to increase further in England and the Netherlands, due to reduced titration with NO. On the other hand, no further increase is expected around Ukraine between 2005 and 2020 as predicted for the period between 1990 and 2005 (see Fig. 7, upper panel). A decrease of about 5-7% is predicted over the Alpine regions and the southern part of the Alps, while ozone is predicted to increase by about 1 ppb (3%) at urban sites (Fig. 9b). One has to keep in mind, however, that the background ozone levels in these simulations were assumed to stay constant between 2005 and 2020, based on the study of Logan et al. (2012).

3.4 AOT40 and SOMO35

The modelled AOT40 and SOMO35 results for the reference year (2005) are shown in Fig. 10. AOT40 values range between 5–30 ppm h, with elevated levels in southern Europe. The SOMO35 values show a similar spatial distribution, lying between 1000 - 5000 ppb d. In Switzerland, the modelled AOT40 is 10-15 ppm h and 20-30 ppm h in the north and south, respectively (Fig. 11, upper panel). We predicted SOMO35 values between 2400-2800 ppb d for northern Switzerland and 4000-4800 ppb d for the southern part of the Alps (Fig. 11, lower panel). These results match very well the AOT40 and SOMO35 values derived from measurements in 2005 (Table 3). Compared to an EMEP model study which reported average AOT40 and SOMO35 of 35.1 ppm h and 5303 ppb d, respectively for Switzerland in 2005 (Gauss et al., 2012), our results are lower and in better agreement with the measurements.

A comparison of simulations for 1990 and 2005 suggests that AOT40 and SOMO35 have decreased in Switzerland since 1990 (Fig. 12), although average annual ozone

mixing ratios increased (Fig. 7). This indicates that peak ozone values decreased due to emission reductions, as shown in Table 4. Although measurements also show a decrease at rural sites, they suggest that AOT40 and SOMO35 increased significantly at urban sites (Table 3). This discrepancy between the model results and observations indicates the sensitivity of these indicator parameters to threshold values. Overestimation of ozone concentrations by regional models at night in polluted urban areas is a common problem. This alone however, cannot be responsible for the discrepancy between measured and modelled AOT40, because AOT40 is the sum of ozone concentrations above 40 ppb and is calculated only during the daytime. The difference between the modelled and measured frequency distributions of ozone mixing ratios above 30-40 ppb is relevant to an understanding of the changes in AOT40 and SOMO35 (Fig. 8). The discrepancy between the modelled and measured relative change in damage indicators is most likely due to the background ozone levels, but this needs further analysis.

Assuming constant background ozone after 2005, AOT40 and SOMO35 were predicted to decrease substantially by 2020 (Figs. S5-S8 of the Supplement). One must keep in mind, however, that these indicators depend strongly on the threshold values, which might be affected by the background ozone and its evolution in the future.

3.5 Nitrogen deposition

The atmospheric deposition of pollutants raises serious concerns for ecosystems. In Switzerland, emissions of air pollutants such as sulphur dioxide and nitrogen oxides have been substantially reduced in the last couple of decades. While sulphur emissions are now stabilized at lower levels than in the past, nitrogen oxide emissions are still rather high. In this section, therefore, we focus on nitrogen deposition.

In general, the main nitrogen sources are emissions of nitrogen oxides from combustion processes and ammonia from agricultural activities. The deposition of atmospheric nitrogen species constitutes a major nutrient input to the biosphere, which enhances forest growth. Despite this, increased nitrogen input into terrestrial ecosystems represents a potential threat to forests. Enhanced nitrogen deposition can cause soil acidification, eutrophication and nutrient imbalances, causing a reduction in biodiversity. The deposition of atmospheric nitrogen compounds occurs via dry and wet processes. NO_2, NH_3, nitric acid (HNO_3), and nitrous acid (HONO) are the most important contributors to nitrogen dry deposition. Nitrogen wet deposition results from the scavenging of atmospheric N constituents.

The predicted annual deposition of total nitrogen in Europe varies between 5 and 45 kg N ha^{-1} y^{-1} in 2006 (Fig. 13, upper panel) and it is mainly dominated by dry deposition (Fig. S9 of the Supplement). Dry deposition is generally largest over regions with large ambient NH_3 concentrations over the Netherlands and Belgium as also reported in the literature (Flechard et al., 2011). We also predict high nitrogen dry deposition around the Po Valley in northern Italy. The modelled total nitrogen deposition varies between 10 and 45 kg N ha^{-1} y^{-1} in northern Switzerland (Fig. 13, lower panel). Elevated levels can also be seen in the south (10-20 kg N ha^{-1} y^{-1}). On the other hand, they are lower at high-altitude sites (about 5 kg N ha^{-1} y^{-1}). These numbers are in the same range as those based on measurements at various locations in Switzerland (Schmitt et al., 2005). In a recent study, Roth et al. (2013) reported an average N deposition on 122 plots in Switzerland of 18.3 kg N ha^{-1} y^{-1} for the year 2007.

Deposition of oxidized and reduced nitrogen species for 2006 is shown in Figs. 14 and 15 for the European and Swiss domains, respectively. The calculated deposition of reduced nitrogen compounds is higher than that of oxidized species. Deposition of

reduced N species - especially NH_3 dry deposition - is high in central Switzerland, where the ammonia emissions are the highest in the country. The combination of high ammonia concentrations and land use favourable for dry deposition leads to the highest deposition of ammonia in the nested domain in a few grid cells in central Switzerland.

A comparison of the simulations for 1990 and 2005 suggests that nitrogen deposition decreased mainly in the eastern part of the European domain, while it increased in the Iberian Peninsula (Fig. 16, upper panel). In Switzerland, the decrease in nitrogen deposition was mainly over the Alpine regions and the southern part of the country (Fig. 16, lower panel). The decrease in nitrogen deposition is mainly related to the oxidized fraction, due to large reductions in NO_x emissions that occurred in the past.

The future simulations assuming the BL 2020 scenario suggest that the oxidized nitrogen deposition will decrease further by about 40% in all of Europe until 2020, whereas deposition of reduced nitrogen compounds will continue to increase by about 20% especially in the southern and eastern part of Europe (Fig. 17). This would lead to a 10 - 20% decrease in the total nitrogen deposition in most of the model domain, with a 10% increase in the eastern part of Europe.

4 Conclusions

The results presented in this study give an overview on predicted nitrogen deposition and the concentrations of ozone and particulate matter in Europe for the past, the present, and different emission scenarios for 2020. They also indicate the importance of the background ozone concentrations in Europe for use in calculating AOT40 and SOMO35 trends.

The modelled relative decreases of the annual average $PM_{2.5}$ concentrations between 1990 and 2005 were 20% and 50% in Europe. Although $PM_{2.5}$ observations were not available for the entire time period, PM_{10} and more recent $PM_{2.5}$ measurements support the modelled trends. In order to have a quantitative evaluation however, it would be advantageous to run and evaluate the model for several years when significant measurement data is available. Among the three Gothenburg scenarios for 2020 (BL, MID and MTFR), the BL scenario is the closest to the recently revised Gothenburg Protocol. Our results show that the application of emission reductions according to the BL scenario would lead to a significant decrease of $PM_{2.5}$ (~30%) in 2020 compared to 2005. The largest predicted decrease in $PM_{2.5}$ based on the MTFR scenario was about 50%-60%, especially in the eastern part of Europe; although its implementation before 2020 is unlikely.

Observations show that mean ozone concentrations did not decrease, but actually increased further in certain areas, in spite of large reductions in European emissions between 1990 and 2005. The model predictions also suggest a similar trend, but the predicted increase is lower than the measured one. This indicates the importance of background ozone. We showed that peak ozone values decreased due to emission reductions whereas ozone levels in polluted regions increased due to reduced titration with NO. The modelled damage indicators AOT40 and SOMO35 for 2005 are in the same range as the measurements. The change in these indicator values between 1990 and 2005, however, did not match the observations. The model results suggest a significant decrease in the indicator levels since 1990. The observations, on the other hand, indicate a decrease at rural sites, but an increase at urban sites. Since the AOT40 and SOMO35 values are very sensitive to the threshold values, the background ozone concentrations might affect the results. We conclude that even though the change in the background ozone used in the model between 1990 and 2005 were adjusted to the recent observations, they might need further revision.

We predicted that the annual average ozone values will continue to increase in the future, by applying the three emission scenarios (BL, MID, MTFR) for 2020. Assuming a constant background ozone levels after 2005, AOT40 and SOMO35 were predicted to decrease by large amounts until 2020 with respect to the reference year 2005. These results, however, have high uncertainty.

We also analysed the model results for both dry and wet deposition of all oxidized and reduced nitrogen species. The annual deposition of total nitrogen in Europe was predicted to vary between 5 - 45 kg N ha^{-1} y^{-1} in 2006 and it was mainly dominated by dry deposition. Dry deposition was generally largest over regions with large ambient NH_3 concentrations over the Netherlands, Belgium and the Po Valley. The modelled annual nitrogen deposition is in the same range as those based on measurements. The predicted annual nitrogen deposition in northern Switzerland varied between 10 - 45 kg N ha^{-1} y^{-1}. Deposition of reduced N species - especially NH_3 dry deposition - is high in central Switzerland, where the ammonia emissions are the highest in the country. The combination of high ammonia concentrations and land use favourable for dry deposition leads to the highest deposition of ammonia in central Switzerland.

Our model results suggest that the nitrogen deposition decreased by 10-30% in the eastern part of Europe between 1990 and 2005, whereas it increased in the Iberian Peninsula. Further reductions in emissions until 2020, according to the baseline scenario, would lead to about 40% lower oxidized nitrogen deposition - mainly due to a reduction in the oxidized fraction - while deposition of reduced nitrogen compounds would continue to increase in most of Europe.

5 Acknowledgements

This study was financially supported by the Swiss Federal Office of Environment, FOEN. We are grateful to the following people and institutions for providing weather, emission and air quality data: ECMWF, TNO, AQMEII, IIASA, INFRAS, Meteotest, NABEL/EMPA. We appreciate the availability of CAMx model developed by ENVIRON. We thank also G. Pirovano and M. Tinguely for providing us with the post-processing tools. Our thanks are extended to G. Theis and R. Weber (FOEN) for the fruitful co-operation throughout this project.

6 References

Aksoyoglu, S., Keller, J., Barmpadimos, I., Oderbolz, D., Lanz, V. A., Prévôt, A. S. H., and Baltensperger, U.: Aerosol modelling in Europe with a focus on Switzerland during summer and winter episodes, Atmos. Chem. Phys., 11 doi:10.5194/acp-5111-7355-2011, 7355-7373, 2011.

Aksoyoglu, S., Keller, J., Oderbolz, D. C., Barmpadimos, I., Prévôt, A. S. H., and Baltensperger, U.: Sensitivity of ozone and aerosols to precursor emissions in Europe, International Journal of Environment and Pollution, 50 451-459, 10.1504/ijep.2012.051215, 2012.

Amann, M., D. Derwent, B. Forsberg, O. Hänninen, F. Hurley, M. Krzyzanowski, F. de Leeuw, S. J. Liu, C. Mandin, J. Schneider, P. Schwarze, and Simpson, D.: Health risks of ozone from long-range transboundary air pollution, edited by: Theakston, F., WHO, Copenhagen,Denmark, 2008.

Andreani-Aksoyoglu, S., and Keller, J.: Estimates of monoterpene and isoprene emissions from the forests in Switzerland, Journal of Atmospheric Chemistry, 20, 71-87, 1995.

Andreani-Aksoyoglu, S., Keller, J., Ordonez, C., Tinguely, M., Schultz, M., and Prévôt, A. S. H.: Influence of various emission scenarios on ozone in Europe, Ecological Modelling, 217, doi:10.1016/j.ecolmodel.2008.06.022, 209-218, 2008.

Ashmore, M. R., and Wilson, R. B.: Critical levels of air pollutants for Europe. Background papers prepared for the United Nations Economic Commission for Europe Workshop on Critical Levels. Egham, United Kingdom, 23-26 March 1992, 1992.

Barmpadimos, I., Hueglin, C., Keller, J., Henne, S., and Prévôt, A. S. H.: Influence of meteorology on PM10 trends and variability in Switzerland from 1991 to 2008, Atmos. Chem. Phys., 11 1813-1835, 2011.

Barmpadimos, I., Keller, J., Oderbolz, D., Hueglin, C., and Prévôt, A. S. H.: One decade of parallel fine (PM2.5) and coarse (PM10–PM2.5) particulate matter measurements in Europe: trends and variability, Atmos. Chem. Phys., 12 3189-3203, 10.5194/acp-12-3189-2012, 2012.

Bergström, R., Denier van der Gon, H. A. C., Prévôt, A. S. H., Yttri, K. E., and Simpson, D.: Modelling of organic aerosols over Europe (2002-2007) using a volatility basis set (VBS) framework: application of different assumptions regarding the formation of secondary organic aerosol Atmos. Chem. Phys., 12 8499-8527, 10.5194/acp-12-8499-2012, 2012.

Colette, A., Granier, C., Hodnebrog, O., Jakobs, H., Maurizi, A., Nyiri, A., Bessagnet, B., D'Angiola, A., D'Isidoro, M., Gauss, M., Meleux, F., Memmesheimer, M., Mieville, A., Rouil, L., Russo, F., Solberg, S., Stordal, F., and Tampieri, F.: Air quality trends in Europe over the past decade: a first multi-model assessment, Atmos. Chem. Phys., 11 11657-11678, 2011.

Cox, R., Bauer, B. L., and Smith, T.: A Mesoscale Model Intercomparison, Bulletin of the American Meteorological Society, 79, 265-283, 10.1175/1520-0477(1998)079<0265:ammi>2.0.co;2, 1998.

Cui, J., Pandey Deolal, S., Sprenger, M., Henne, S., Staehelin, J., Steinbacher, M., and Nédélec, P.: Free tropospheric ozone changes over Europe as observed at Jungfraujoch (1990–2008): An analysis based on backward trajectories, Journal of Geophysical Research: Atmospheres, 116, D10304, 10.1029/2010jd015154, 2011.

Cusack, M., Alastuey, A., Pérez, N., Pey, J., and Querol, X.: Trends of particulate matter (PM2.5) and chemical composition at a regional background site in the Western Mediterranean over the last nine years (2002–2010), Atmos. Chem. Phys., 12 8341-8357, 10.5194/acp-12-8341-2012, 2012.

Denier van der Gon, H., Visschedijk, A., van de Brugh, H., and Droege, R.: A high resolution European emission data base for the year 2005. A contribution to UBA-Projekt: “Strategien zur Verminderung der Feinstaubbelastung” – PAREST: Partikelreduktionsstrategien –Particle Reduction Strategies TNO, Utrecht (NL)TNO-034-UT-2010-01895_RPT-ML, 2010.

Engler, C., Birmili, W., Spindler, G., and Wiedensohler, A.: Analysis of exceedances in the daily PM10 mass concentration (50 µg m−3) at a roadside station in Leipzig, Germany, Atmos. Chem. Phys., 12 10107-10123, 10.5194/acp-12-10107-2012, 2012.

Flechard, C. R., Nemitz, E., Smith, R. I., Fowler, D., Vermeulen, A. T., Bleeker, A., Erisman, J. W., Simpson, D., Zhang, L., Tang, Y. S., and Sutton, M. A.: Dry deposition of reactive nitrogen to European ecosystems: a comparison of inferential models across the NitroEurope network, Atmos. Chem. Phys., 11 2703-2728, 10.5194/acp-11-2703-2011, 2011.

Gauss, M., A. Nyiri, B.M. Steensen, and Klein, H.: Transboundary air pollution by main pollutants (S, N, O3) and PM in 2010 Switzerland, Norway, ISSN 1890-0003, 2012.

Heldstab, J., de Haan van der Weg, P., Kuenzle, T., Keller, M., and Zbinden, R.: Modelling of PM10 and PM2.5 ambient concentrations in Switzerland 2000 and 2010 Bundesamt fuer Umwelt, Wald und Landschaft (BUWAL), Bern, Environmental Documentation No. 169, 2003.

Heldstab, J., and Wuethrich, P.: Emissionsmuster. Raeumliche Verteilung und Ganglinien fuer CO- /NMVOC-Emissionen BAFU, Bern / Zürich, 15, 2006.

Hettelingh, J.-P., Posch, M., Velders, G. J. M., Ruyssenaars, P., Adams, M., de Leeuw, F., Lükewille, A., Maas, R., Sliggers, J., and Slootweg, J.: Assessing interim objectives for acidification, eutrophication and ground-level ozone of the EU National Emission Ceilings Directive with 2001 and 2012 knowledge, Atmospheric Environment, 75, 129-140, http://dx.doi.org/10.1016/j.atmosenv.2013.03.060, 2013.

Horowitz, L. W., Walters, S., Mauzerall, D. L., Emmons, L. K., Rasch, P. J., Granier, C., Tie, X., Lamarque, J.-F., Schultz, M. G., Tyndall, G. S., Orlando, J. J., and Brasseur, G. P.: A global simulation of tropospheric ozone and related tracers: Description and evaluation of MOZART, version 2. , J. Geophys. Res., 108, doi:10.1029/2002JD002853., 2003.

INFRAS: HBEFA. Handbuch Emissionsfaktoren des Strassenverkehrs. Version 3.1, INFRAS, UBA Berlin, UBA Wien, BAFU, Bern, 2010.

Kropf, R.: Massnahmen zur Reduktion der PM10-Emissionen Bundesamt fuer Umwelt (BAFU), BernUmwelt-Materialien Nr. 136, Luft, 112, 2001.

Kupper, T., Bonjour, C., Achermann, B., Zaucker, F., Rihm, B., Nyfeler-Brunner, A., Leuenberger, C., and Menzi, H.: Ammoniakemissionen in der Schweiz: Neuberechnung 1990-2007 Prognose bis 2020 BAFU, 2010.

Lanz, V. A., Prévôt, A. S. H., Alfarra, M. R., Weimer, S., Mohr, C., DeCarlo, P. F., Gianini, M. F. D., Hueglin, C., Schneider, J., Favez, O., D'Anna, B., George, C., and Baltensperger, U.: Characterization of aerosol chemical composition with aerosol mass spectrometry in Central Europe: an overview, Atmos. Chem. Phys., 10 10453-10471, 2010.

Logan, J. A., Staehelin, J., Megretskaia, I. A., Cammas, J. P., Thouret, V., Claude, H., De Backer, H., Steinbacher, M., Scheel, H. E., Stübi, R., Fröhlich, M., and Derwent, R.: Changes in ozone over Europe: Analysis of ozone measurements from sondes, regular aircraft (MOZAIC) and alpine surface sites, J. Geophys. Res., 117 D09301, 10.1029/2011jd016952, 2012.

Madronich, S.: The Tropospheric Visible Ultra-violet (TUV) model web page. , National Center for Atmospheric Research, Boulder, CO. , http://www.acd.ucar.edu/TUV/, 2002.

Mahrer, F., and Vollenweider, C.: Landesforstinventar LFI, Eidgenössische Forschungsanstalt für Wald, Schnee und Landschaft (WSL), Birmensdorf, 1983.

NASA/GSFC, Total ozone mapping spectrometer: http://toms.gsfc.nasa.gov/ozone/ozone.html, 2005.

Oderbolz, D. C., Aksoyoglu, S., Keller, J., Barmpadimos, I., Steinbrecher, R., Skjøth, C. A., Plaß-Dülmer, C., and Prévôt, A. S. H.: A comprehensive emission inventory of biogenic volatile organic compounds in Europe: improved seasonality and land-cover, Atmos. Chem. Phys., 13 1689-1712, 10.5194/acp-13-1689-2013, 2013.

Ordonez, C., Brunner, D., Staehelin, J., Hadjinicolaou, P., Pyle, J. A., Jonas, M., Wernli, H., and Prévôt, A. S. H.: Strong Influence of lowermost stratospheric ozone on lower tropospheric background ozone changes over Europe, Geophysical Research Letters, 34 doi:10.1029/2006GL029113, 2007.

Roth, T., Kohli, L., Rihm, B., and Achermann, B.: Nitrogen deposition is negatively related to species richness and species composition of vascular plants and bryophytes in Swiss mountain grassland, Agriculture, Ecosystems & Environment, 178, 121-126, http://dx.doi.org/10.1016/j.agee.2013.07.002, 2013.

Schmitt, M., Thöni, L., Waldner, P., and Thimonier, A.: Total deposition of nitrogen on Swiss long-term forest ecosystem research (LWF) plots: comparison of the throughfall and the inferential method, Atmospheric Environment, 39 1079-1091, http://dx.doi.org/10.1016/j.atmosenv.2004.09.075, 2005.

Schneider, A.: Branchenspezifische VOC-Profile BAFU, Bern / Basel, 129.17, 2007.

Simpson, D., Winiwarter, W., Börjesson, G., Cinderby, S., Ferreiro, A., Guenther, A., Hewitt, N. C., Janson, R., Khalil, M. A. K., Owen, S., Pierce, T. E., Puxbaum, H., Shearer, M., Skiba, U., Steinbrecher, R., Tarrasón, L., and Öquist, M. G.: Inventorying emissions from nature in Europe, Journal of Geophysical Research, 104 8113-8152, 1999.

Solazzo, E., Bianconi, R., Vautard, R., Appel, K. W., Moran, M. D., Hogrefe, C., Bessagnet, B., Brandt, J., Christensen, J. H., Chemel, C., Coll, I., Denier van der Gon, H., Ferreira, J., Forkel, R., Francis, X. V., Grell, G., Grossi, P., Hansen, A. B., Jeričević, A., Kraljević, L., Miranda, A. I., Nopmongcol, U., Pirovano, G., Prank, M., Riccio, A., Sartelet, K. N., Schaap, M., Silver, J. D., Sokhi, R. S., Vira, J., Werhahn, J., Wolke, R., Yarwood, G., Zhang, J., Rao, S. T., and Galmarini, S.: Model evaluation and ensemble modelling of surface-level ozone in Europe and North America in the context of AQMEII, Atmospheric Environment, 53, 60-74, http://dx.doi.org/10.1016/j.atmosenv.2012.01.003, 2012a.

Solazzo, E., Bianconi, R., Pirovano, G., Matthias, V., Vautard, R., Moran, M. D., Wyat Appel, K., Bessagnet, B., Brandt, J., Christensen, J. H., Chemel, C., Coll, I., Ferreira, J., Forkel, R., Francis, X. V., Grell, G., Grossi, P., Hansen, A. B., Miranda, A. I., Nopmongcol, U., Prank, M., Sartelet, K. N., Schaap, M., Silver, J. D., Sokhi, R. S., Vira, J., Werhahn, J., Wolke, R., Yarwood, G., Zhang, J., Rao, S. T., and Galmarini, S.: Operational model evaluation for particulate matter in Europe and North America in the context of AQMEII, Atmospheric Environment, 53, 75-92, http://dx.doi.org/10.1016/j.atmosenv.2012.02.045, 2012b.

Tørseth, K., Aas, W., Breivik, K., Fjæraa, A. M., Fiebig, M., Hjellbrekke, A. G., Lund Myhre, C., Solberg, S., and Yttri, K. E.: Introduction to the European Monitoring and Evaluation Programme (EMEP) and observed atmospheric composition change during 1972-2009, Atmos. Chem. Phys., 12 5447-5481, 10.5194/acp-12-5447-2012, 2012.

UNECE: Protocol to Abate Acidification, Eutrophication and Ground-level Ozone http://www.unece.org/env/lrtap/multi_h1.htm, 1999.

Wilson, R. C., Fleming, Z. L., Monks, P. S., Clain, G., Henne, S., Konovalov, I. B., Szopa, S., and Menut, L.: Have primary emission reduction measures reduced ozone across Europe? An analysis of European rural background ozone trends 1996–2005, Atmos. Chem. Phys., 12 437-454, 10.5194/acp-12-437-2012, 2012.

Yarwood, G., Rao, S., Yocke, M., and Whitten, G. Z.: Updates to the Carbon Bond chemical mechanism: CB05 Yocke & Company, Novato, CA 94945RT-04-00675, 2005.

Zhang, L., Brook, J. R., and Vet, R.: A revised parameterization for gaseous dry deposition in air-quality models, Atmos. Chem. Phys., 3 2067-2082, 10.5194/acp-3-2067-2003, 2003.

Zhang, Y., Olsen, S. C., and Dubey, M. K.: WRF/Chem simulated springtime impact of rising Asian emissions on air quality over the U.S, Atmospheric Environment, 44 2799-2812, 2010.

Table 1: Description of emission scenarios

scenario	Description
1990	retrospective analysis
2005	reference year
2006	model validation
2020 BL*	baseline scenario
2020 MID*	mid scenario
2020 MTFR*	maximum technically feasible reduction scenario

- from IIASA/GAINS

Table 2: Statistical quantities for O_3 and $PM_{2.5}$ using rural background stations in the AirBase dataset for 2006 (model output from the European domain).

	O_3 (ppb)		$PM_{2.5}$ ($\mu g\ m^{-3}$)	
	Obs.	model	Obs.	model
Mean	29.5	33.5	13.5	11.6
Standard deviation	11.2	7.9	6.4	4.9
Minimum	10.0	15.1	4.1	2.6
Maximum	70.4	53.9	63.4	41.2
Mean bias	4.0		-1.9	
Correlation coefficient	0.84		0.43	
Number of stations	300		19	

Table 3: Mean O_3, AOT40 and SOMO35 from measurements at NABEL stations in Switzerland (FOEN).

Station	type	O_3 ($\mu g\ m^{-3}$)			AOT40 (ppm h)			SOMO35 (ppb d)		
		1990	2005	% change	1990	2005	% change	1990	2005	% change
Basel	suburban	34.0	47.4	+39	13.6	14.9	+10	2164	2752	+27
Davos	rural, elevated	65.6	70.8	+8	19.8	19.4	-2	3817	4519	+18
Duebendorf	suburban	32.4	43.9	+36	15.0	15.2	+1	2261	2700	+19
Jungfraujoch	mountain	70.2	74.8	+7	39.8	41.6	+5	7014	7969	+14
Lugano	urban	38.1	52.8	+39	23.8	30.0	+26	3740	4672	+25
Lägeren	rural	63.9	69.3	+9	22.4	17.7	-21	4690	3962	-16
Payerne	rural	51.6	56.1	+9	24.8	18.2	-27	4044	3350	-17
Sion	highway	30.0	41.0	+37	12.7	11.7	-8	2504	2516	+1
Tänikon	rural	46.2	55.9	+21	19.8	16.1	-19	3740	3099	-17
Zurich	urban	29.3	44.8	+53	7.5	14.0	+87	1959	2469	+26

Table 4: Measured and modelled peak ozone concentrations at NABEL stations in 1990 and 2005

Station	type	Measured max O_3 ($\mu g\ m^{-3}$)		Modelled max O_3 ($\mu g\ m^{-3}$)	
		1990	2005	1990	2005
Basel	suburban	200	224	180	145
Davos	rural, elevated	142	136	147	123
Duebendorf	suburban	216	212	214	163
Jungfraujoch	mountain	131	130	144	121
Lägeren	rural	217	205	213	160
Lugano	urban	269	255	235	185
Payerne	rural	196	184	175	133
Sion	highway	174	170	138	115
Tänikon	rural	212	199	210	158
Zurich	urban	190	210	213	161

Figure Captions:

Figure 1: Relative changes (%) in annual emissions of SO_2, NO_x, NMVOC, NH_3 and $PM_{2.5}$ with respect to reference year (2005) for various scenarios in Switzerland (CH) and the European countries (EU) (for definition of scenarios see text).

Figure 2: Time series of modelled (CAMx) and measured (AirBase) hourly average O_3 (ppb) (upper panel) and daily average $PM_{2.5}$ ($\mu g\ m^{-3}$) (lower panel) in 2006 (European domain). Number of measurement sites: 300 for O_3, 19 for PM2.5.

Figure 3: Frequency distributions of ozone (upper panel) and PM_{10} (lower panel) at Chaumont (rural) and Zurich (urban background) in 2006.

Figure 4: Measured (red) and modelled (black) hourly concentrations of particulate nitrate, sulphate, ammonium, organic aerosols (OA), elemental carbon (EC) and $PM_{2.5}$ (sum of all species shown above) at Payerne in June 2006. EC was measured by an Aethalometer, the other components by an AMS.

Figure 5: Relative changes in annual average $PM_{2.5}$ concentrations over the European (upper panel) and Swiss (lower panel) domains, 2005-1990.

Figure 6: Relative changes in annual average $PM_{2.5}$ concentrations over the European domain for two scenarios: BL 2020 - 2005 (upper panel) and MTFR 2020 - 2005 (lower panel).

Figure 7: Changes (ppb) in annual average ozone mixing ratios over the European (upper panel) and Swiss (lower panel) domains, 2005 – 1990.

Figure 8: Changes in frequency distributions of measured (left) and modelled (right) ozone between 1990 and 2005 in Zurich.

Figure 9a: Changes in annual average ozone mixing ratios (ppb) over the European domain, BL 2020- 2005 (upper panel), MTFR 2020- 2005 (lower panel).

Figure 9b: Changes in annual average ozone mixing ratios (ppb) over the Swiss domain, BL 2020- 2005 (upper panel), MTFR 2020- 2005 (lower panel).

Figure 10: Modelled AOT40 (ppm h) (upper panel) and SOMO35 (ppb d) (lower panel) over the European domain for the reference year (2005).

Figure 11: Modelled AOT40 (ppm h) (upper panel) and SOMO35 (ppb d) (lower panel) over the Swiss domain for the reference year (2005).

Figure 12: Relative changes in AOT40 (upper panel) and in SOMO35 (lower panel) over the Swiss domain, 2005 – 1990.

Figure 13: Total N deposition (kg N ha^{-1} y^{-1}) over the European (upper panel) and the Swiss (lower panel) domains (2006).

Figure 14: Deposition (kg N $ha^{-1}y^{-1}$) of oxidized (upper panel) and reduced (lower panel) nitrogen compounds over the European domain (2006).

Figure 15: Deposition (kg N $ha^{-1}y^{-1}$) of oxidized (upper panel) and reduced (lower panel) nitrogen compounds over the Swiss domain (2006).

Figure 16: Relative changes in nitrogen deposition over the European (upper panel) and the Swiss (lower panel) domains, 2005 – 1990.

Figure 17: Relative changes in deposition of oxidized (upper panel) and reduced (lower panel) nitrogen species over the European domain, BL 2020 – 2005.

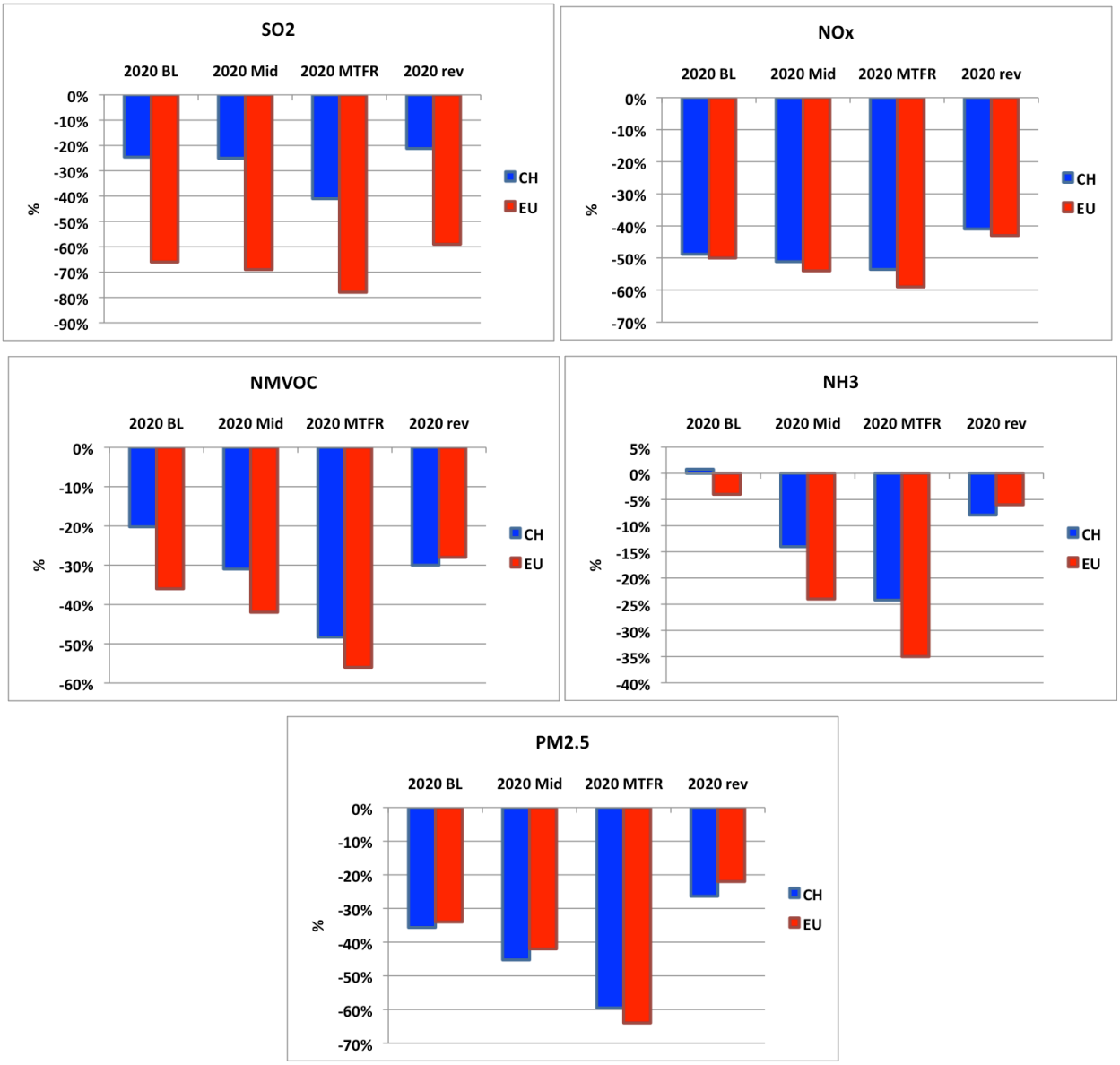

Figure 1: Relative changes (%) in annual emissions of SO_2, NO_x, NMVOC, NH_3 and $PM_{2.5}$ with respect to reference year (2005) for various scenarios in Switzerland (CH) and the European countries (EU) (for definition of scenarios see text).

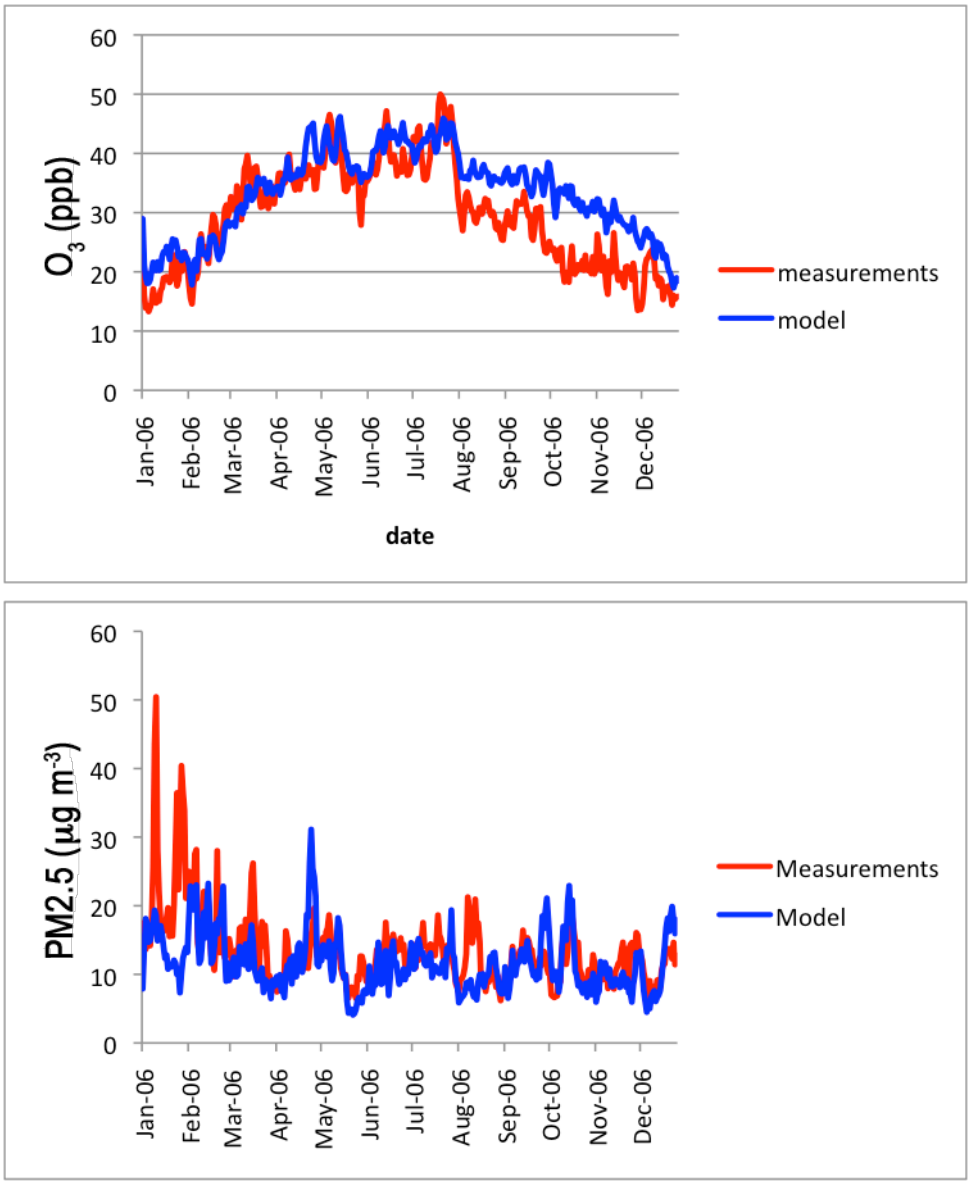

Figure 2: Time series of modelled (CAMx) and measured (AirBase) hourly average O_3 (ppb) (upper panel) and daily average $PM_{2.5}$ (µg m^{-3}) (lower panel) in 2006 (European domain). Number of measurement sites: 300 for O_3, 19 for PM2.5.

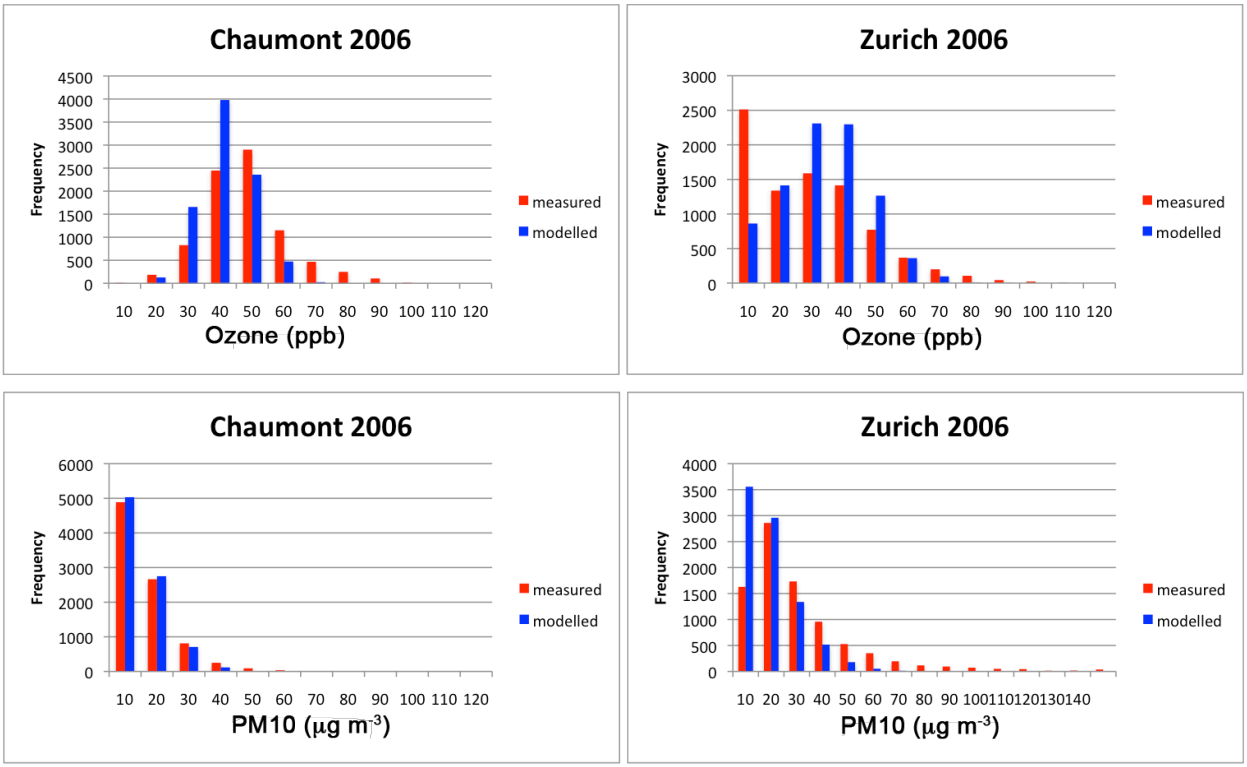

Figure 3: Frequency distributions of ozone (upper panel) and PM_{10} (lower panel) at Chaumont (rural) and Zurich (urban background) in 2006.

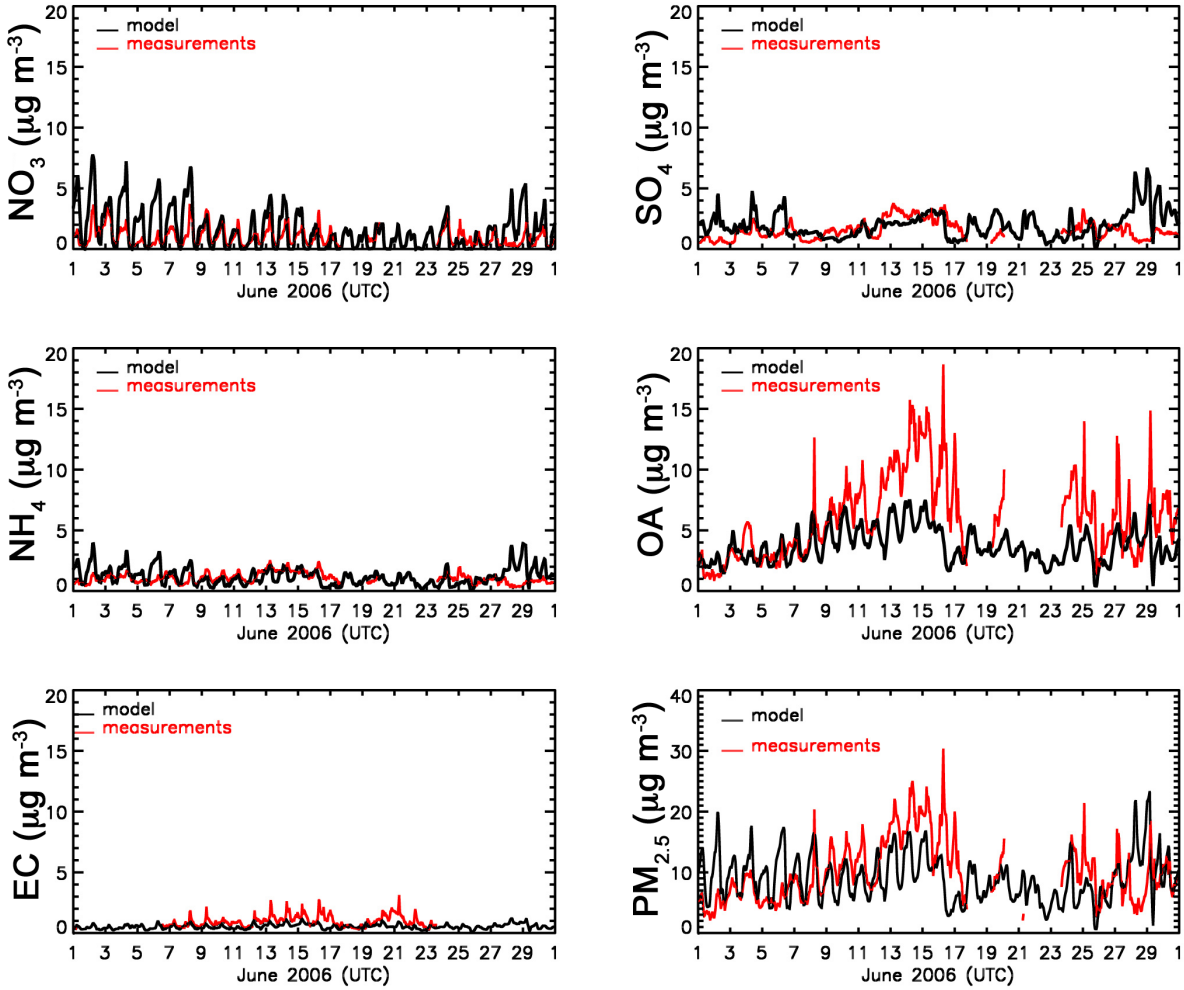

Figure 4: Measured (red) and modelled (black) hourly concentrations of particulate nitrate, sulphate, ammonium, organic aerosols (OA), elemental carbon (EC) and $PM_{2.5}$ (sum of all species shown above) at Payerne in June 2006. EC was derived from Aethalometer measurements, the other components were measured by an AMS.

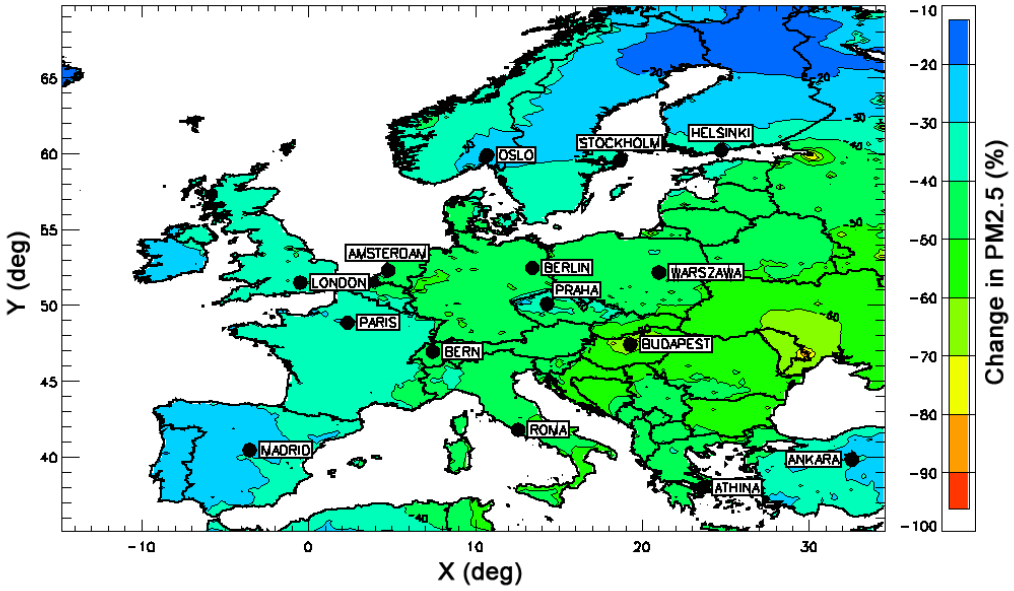

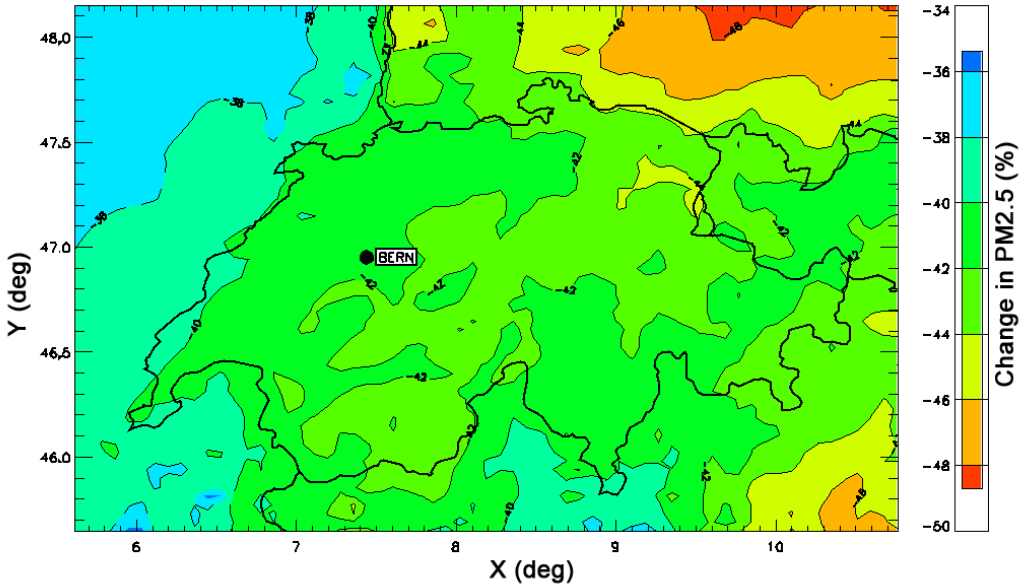

Figure 5: Relative changes in annual average $PM_{2.5}$ concentrations over the European (upper panel) and Swiss (lower panel) domains, 2005-1990.

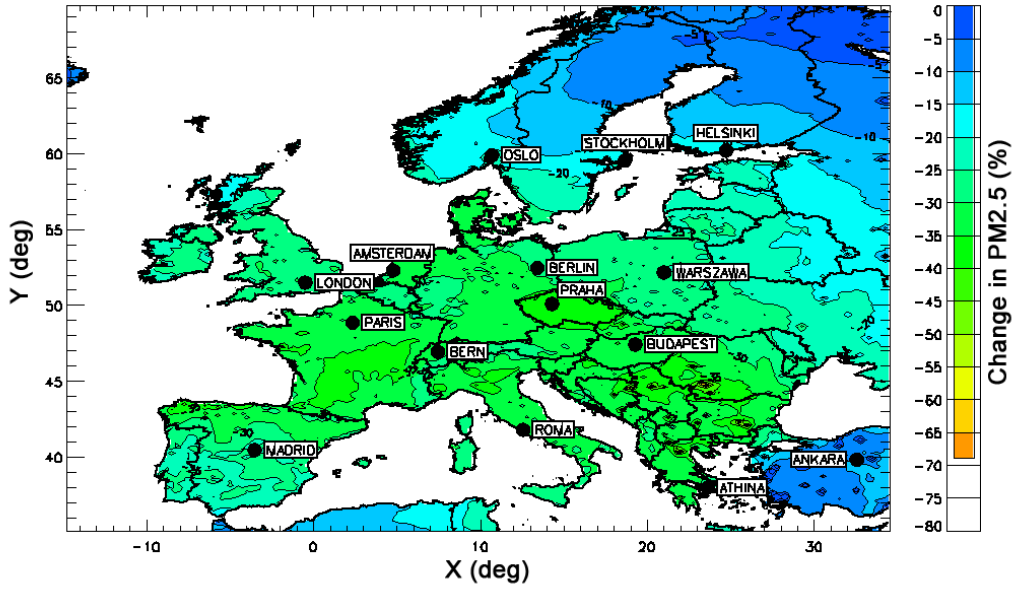

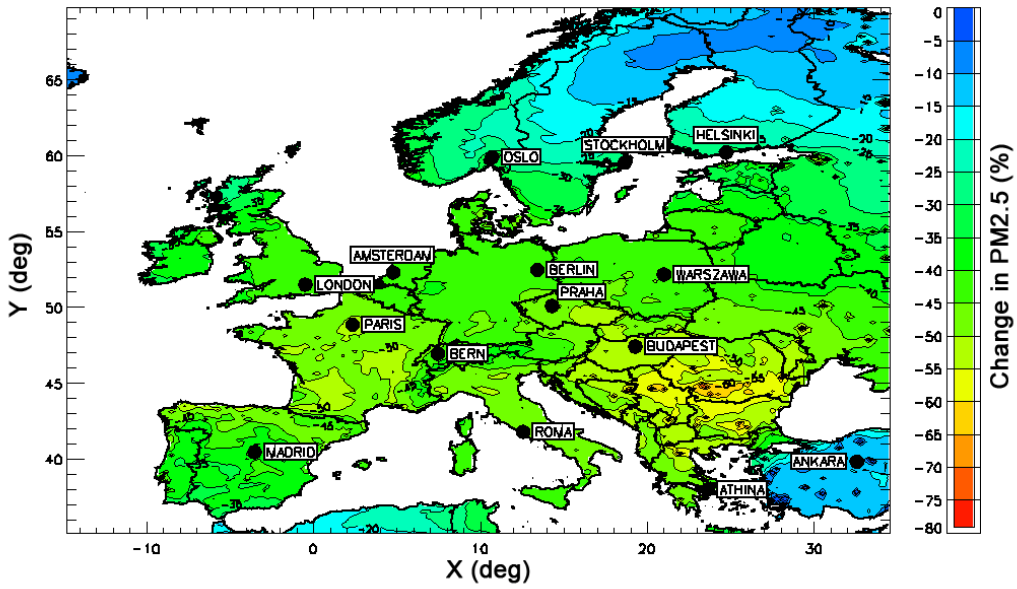

Figure 6: Relative changes in annual average $PM_{2.5}$ concentrations over the European domain for two scenarios: BL 2020 - 2005 (upper panel) and MTFR 2020 - 2005 (lower panel).

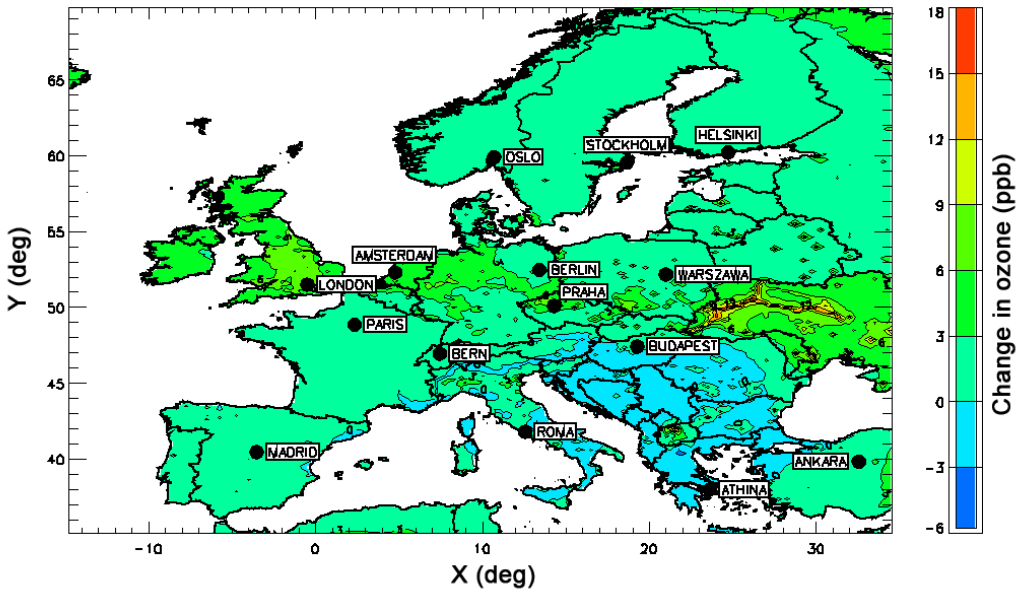

1

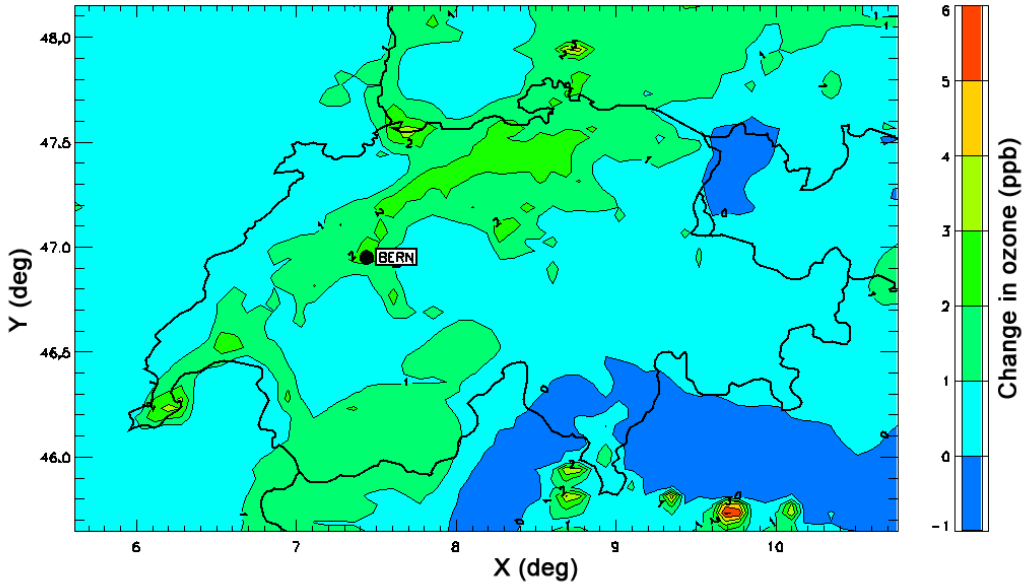

2

3 Figure 7: Changes (ppb) in annual average ozone mixing ratios over the European
4 (upper panel) and Swiss (lower panel) domains, 2005 – 1990.

5

6

7

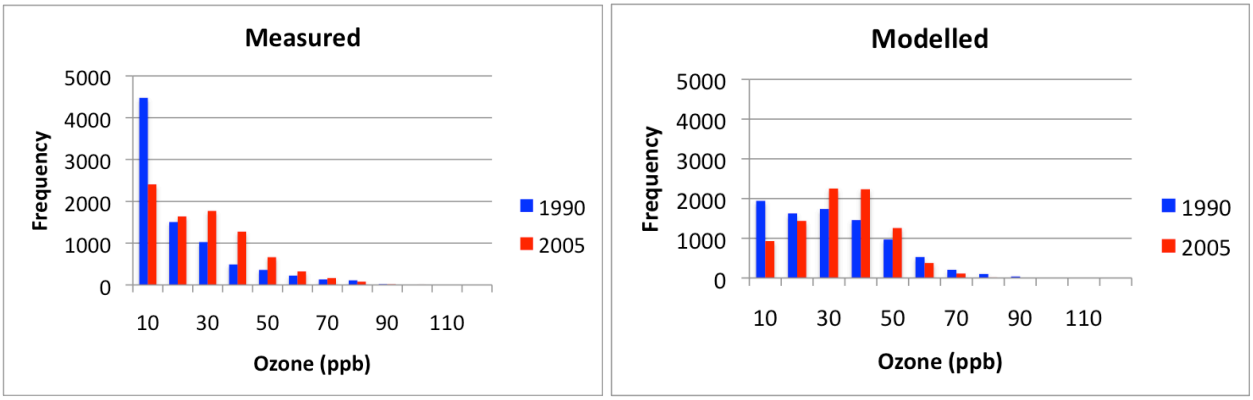

Figure 8: Changes in frequency distributions of measured (left) and modelled (right) ozone between 1990 and 2005 in Zurich.

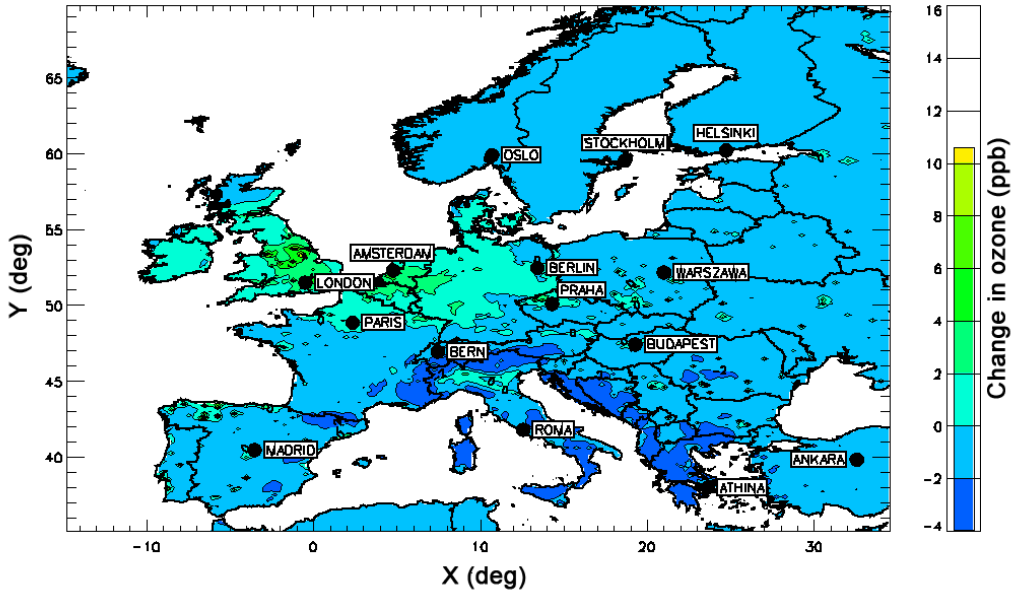

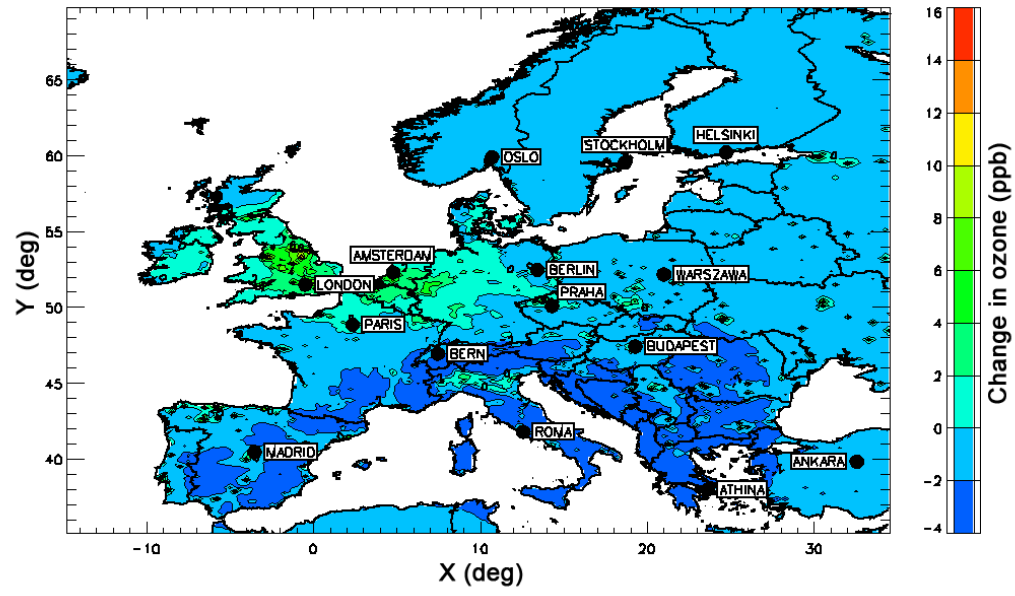

Figure 9a: Changes in annual average ozone mixing ratios (ppb) over the European domain, BL 2020- 2005 (upper panel), MTFR 2020- 2005 (lower panel).

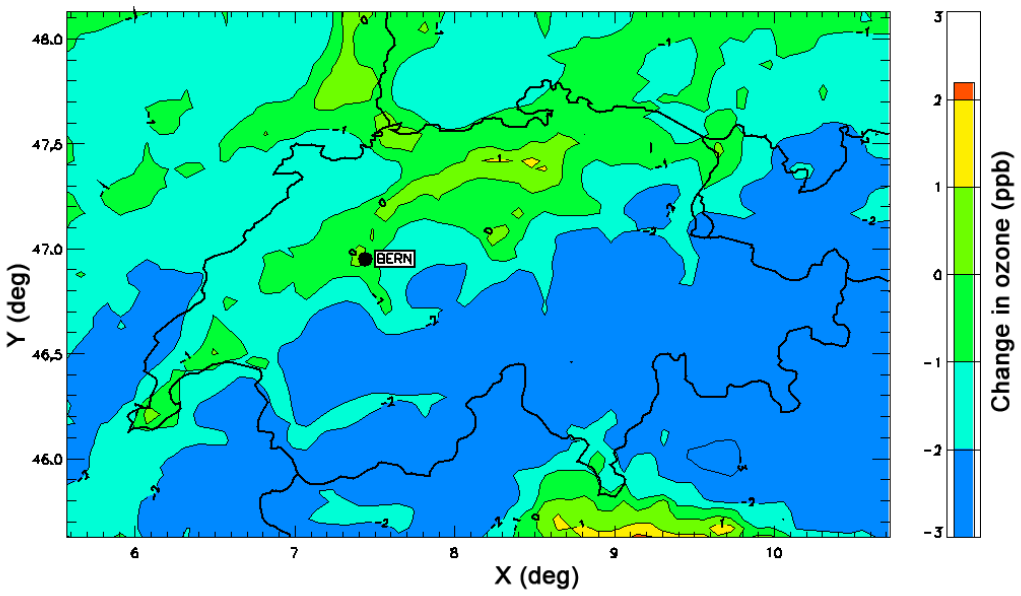

1

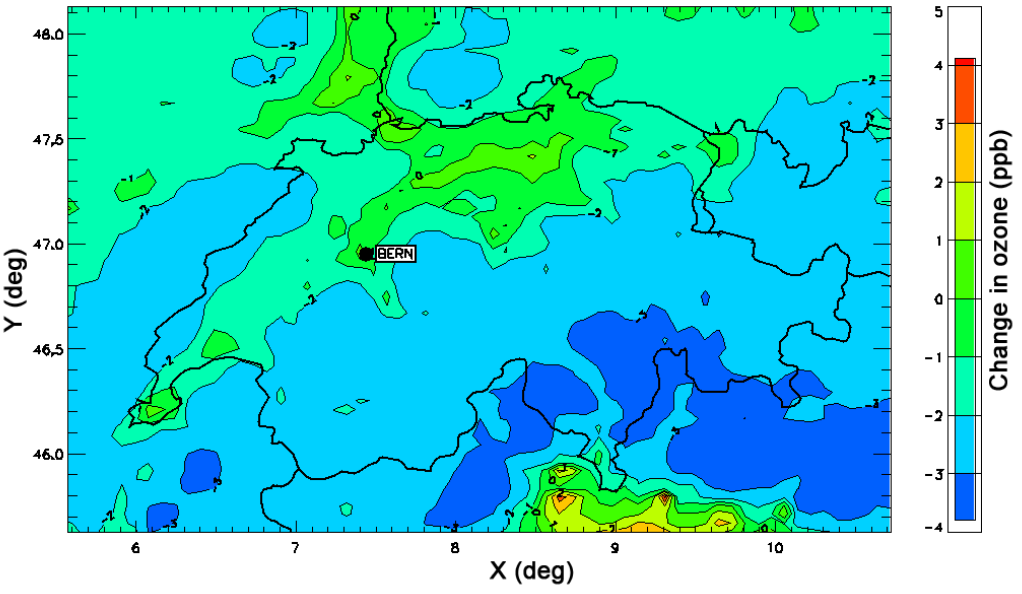

2

3 Figure 9b: Changes in annual average ozone mixing ratios (ppb) over the Swiss domain,
4 BL 2020- 2005 (upper panel), MTFR 2020- 2005 (lower panel).

5

1

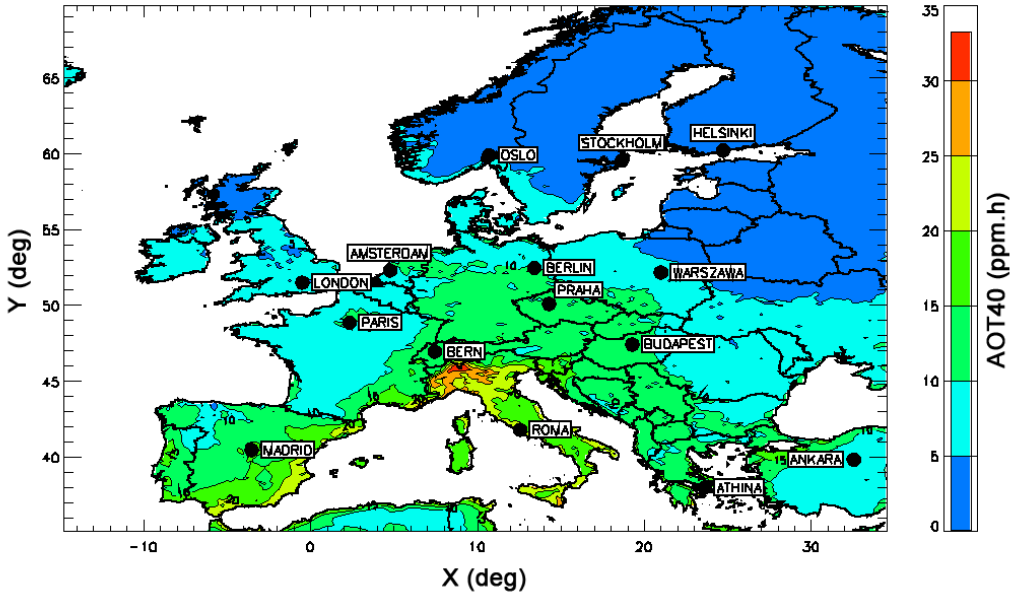

2

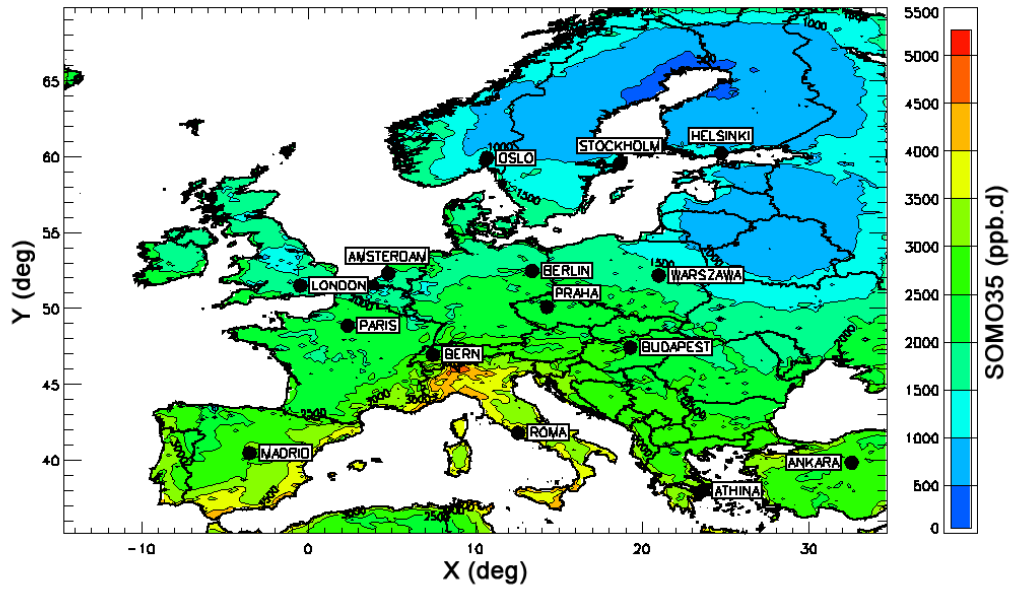

3

4 Figure 10: Modelled AOT40 (ppm h) (upper panel) and SOMO35 (ppb d) (lower panel)
5 over the European domain for the reference year (2005).

6

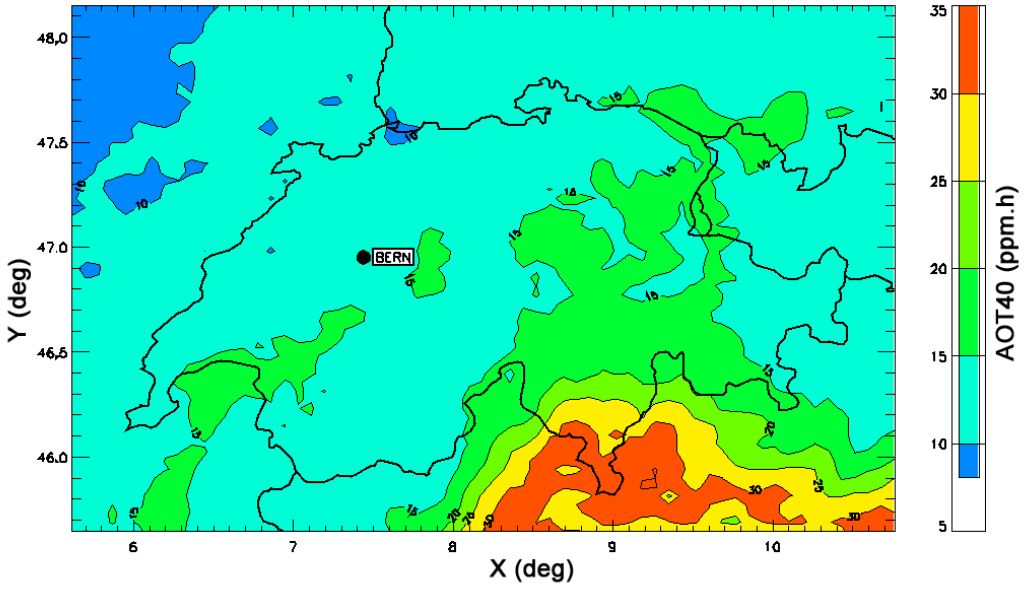

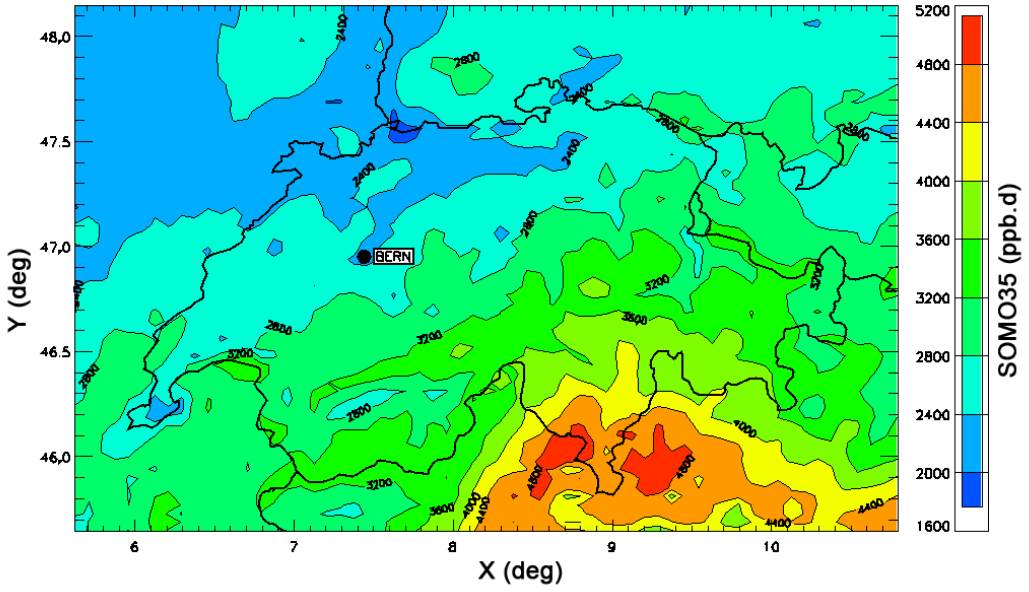

Figure 11: Modelled AOT40 (ppm h) (upper panel) and SOMO35 (ppb d) (lower panel) over the Swiss domain for the reference year (2005).

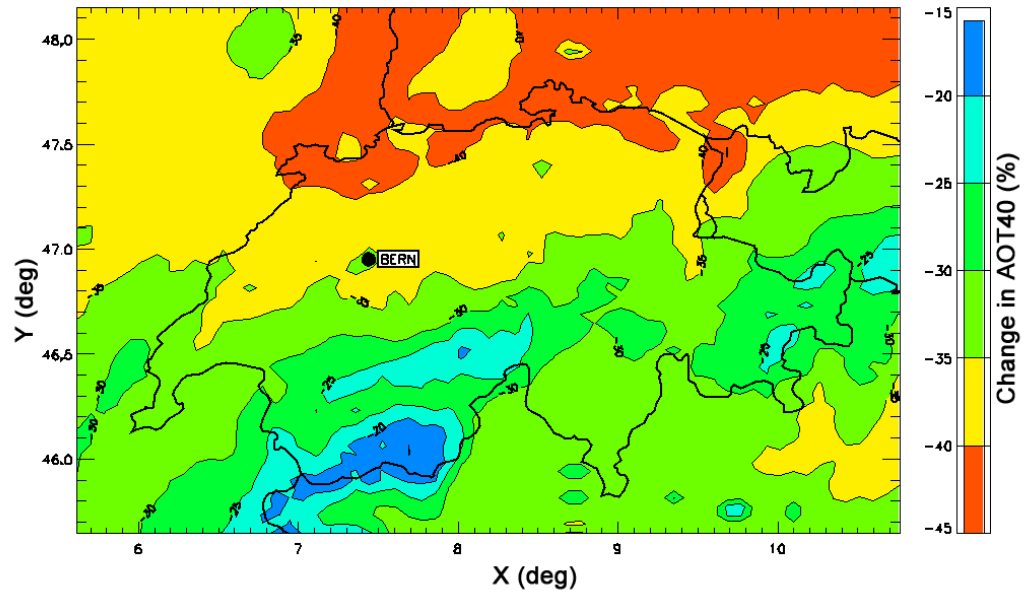

1

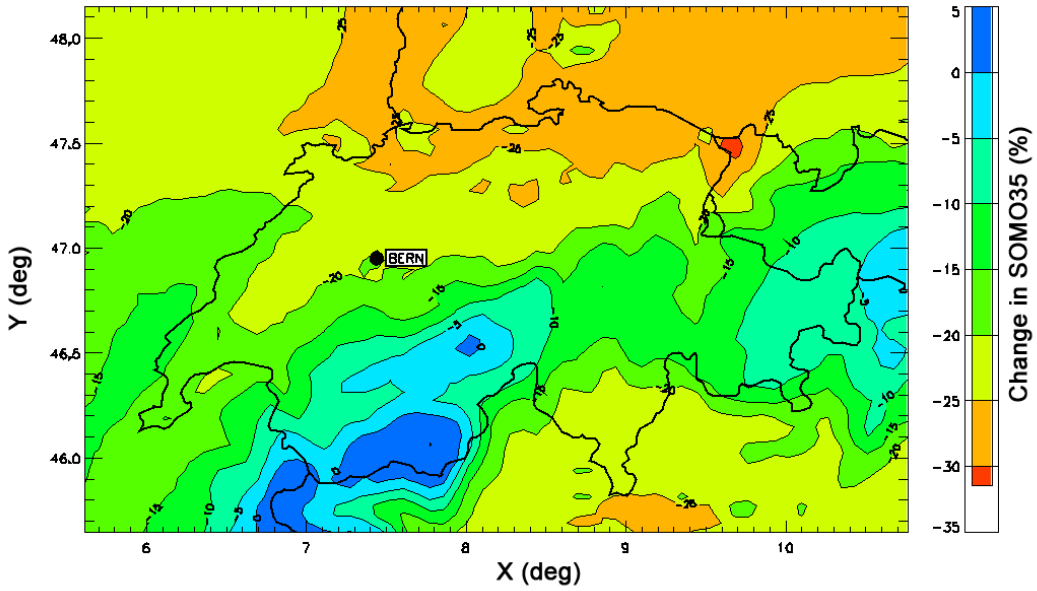

2

3 Figure 12: Relative changes in AOT40 (upper panel) and in SOMO35 (lower panel) over
4 the Swiss domain, 2005 – 1990.

5

6

7

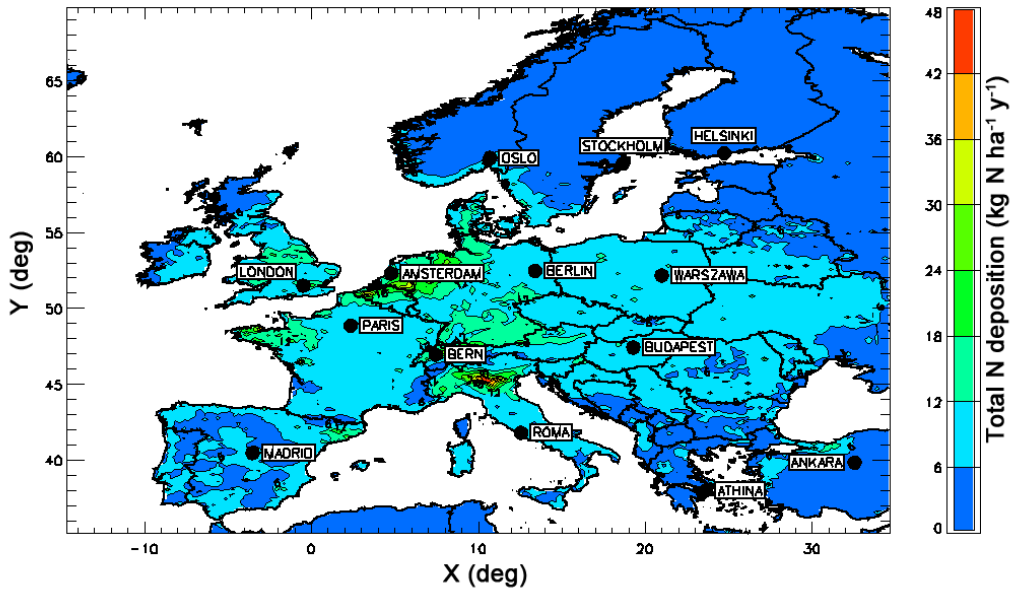

1

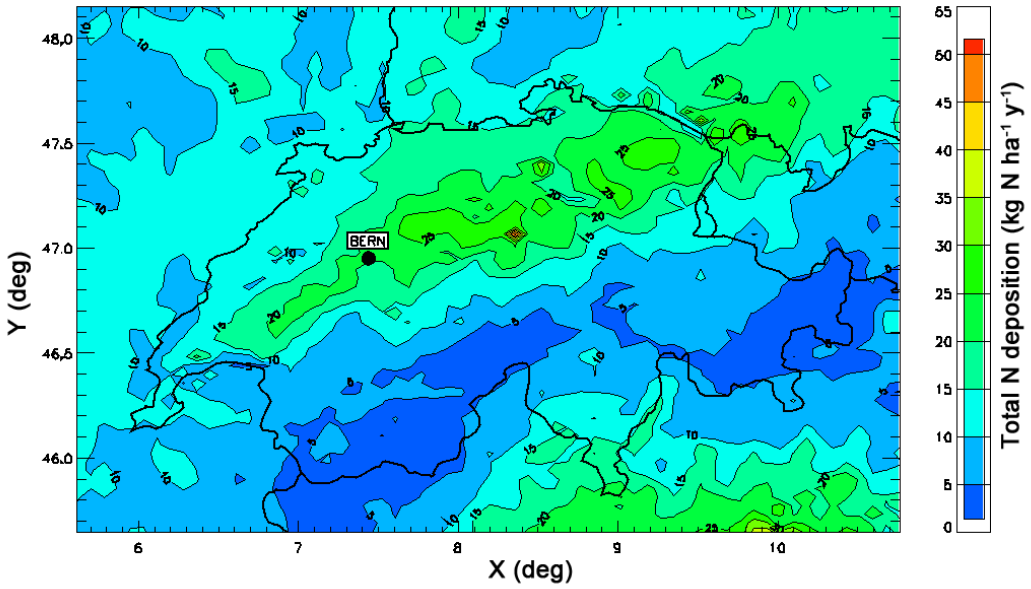

2

3 Figure 13: Total N deposition (kg N ha^{-1} y^{-1}) over the European (upper panel) and the
4 Swiss (lower panel) domains (2006).

5

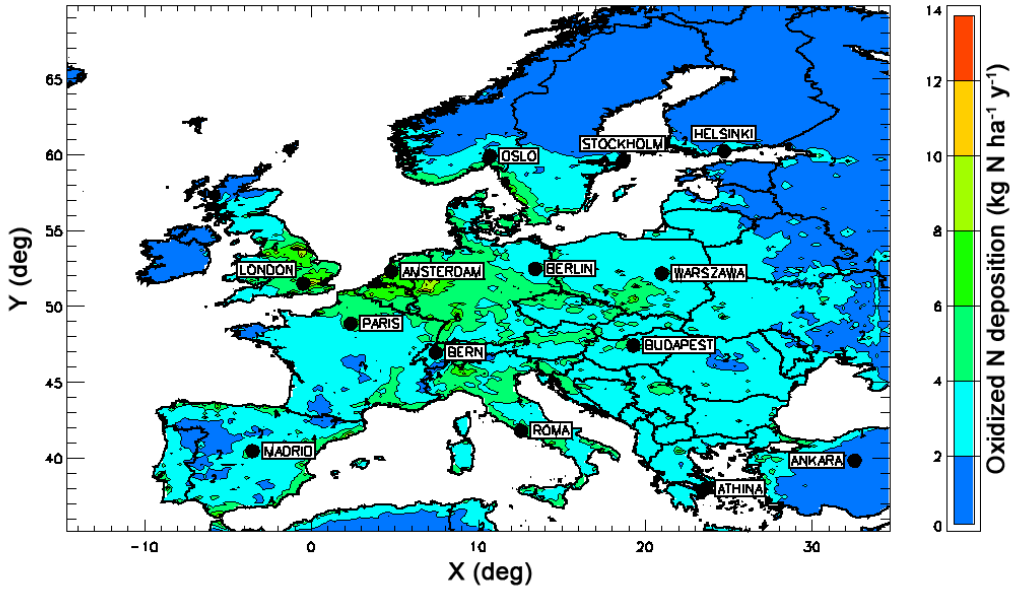

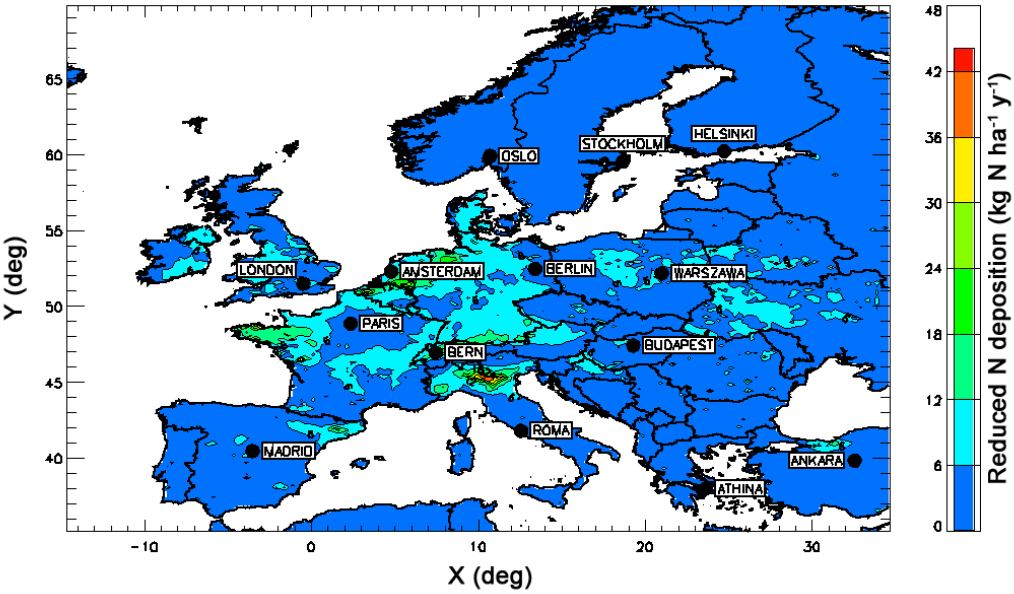

Figure 14: Deposition (kg N $ha^{-1}y^{-1}$) of oxidized (upper panel) and reduced (lower panel) nitrogen compounds over the European domain (2006).

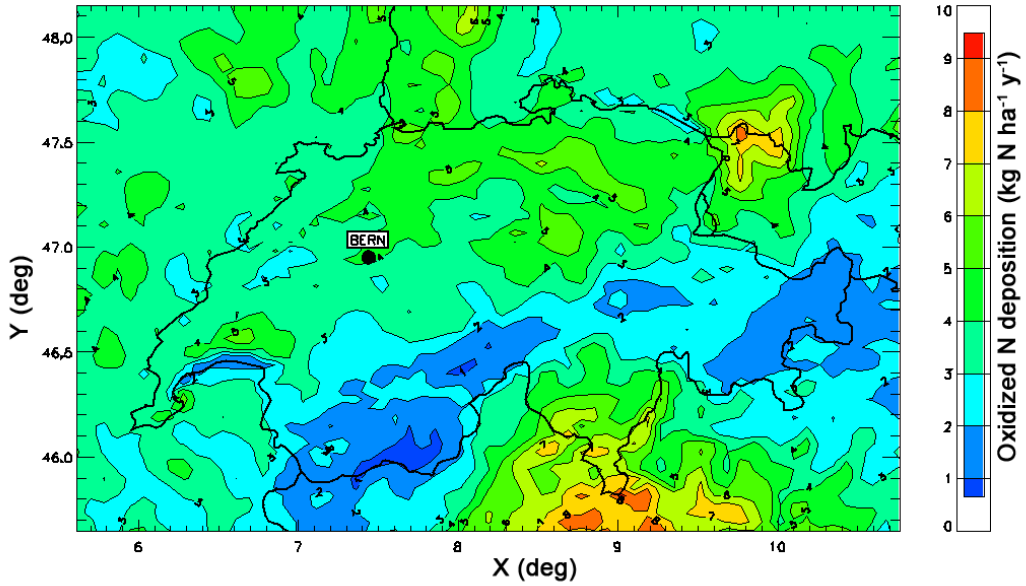

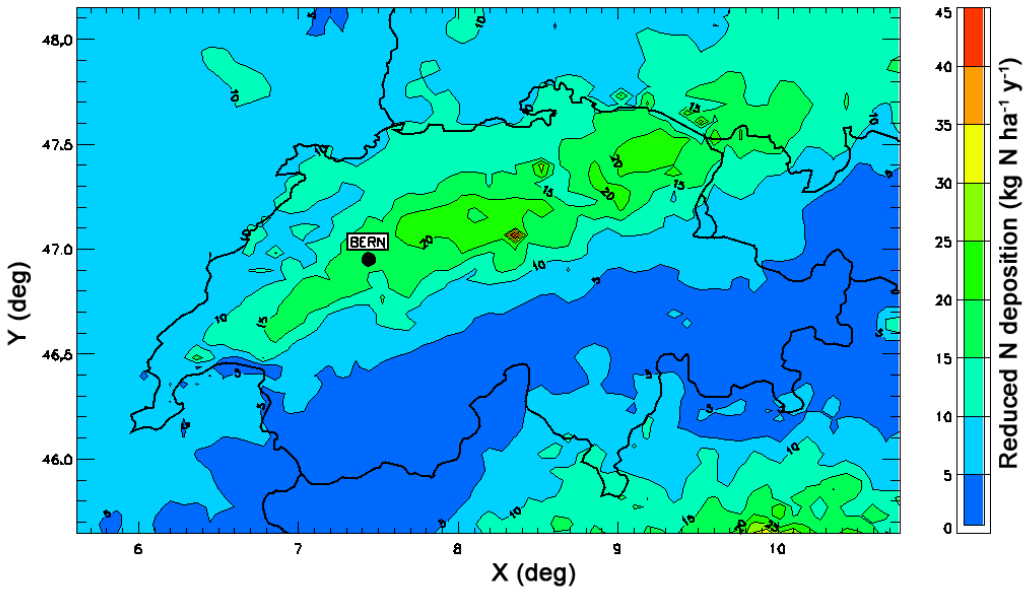

Figure 15: Deposition (kg N $ha^{-1}y^{-1}$) of oxidized (upper panel) and reduced (lower panel) nitrogen compounds over the Swiss domain (2006).

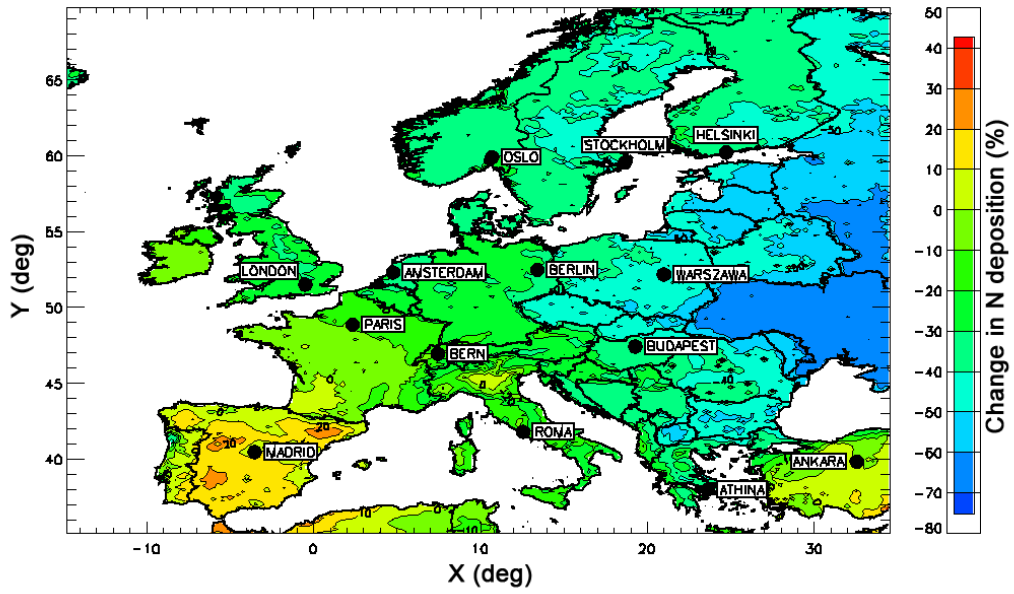

1

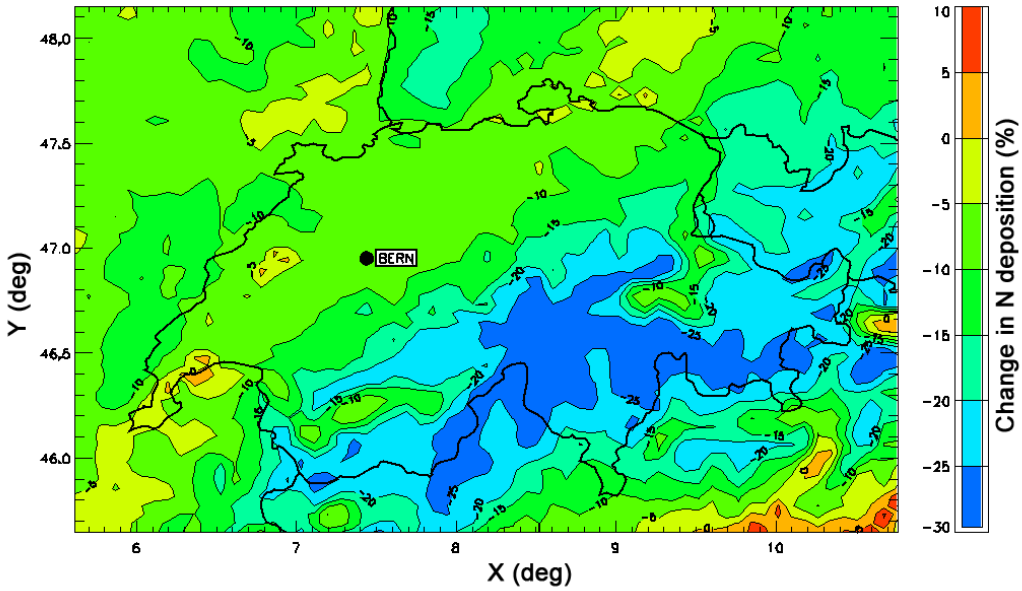

2

3 Figure 16: Relative changes in nitrogen deposition over the European (upper panel) and
4 the Swiss (lower panel) domains, 2005 – 1990.

5

6

7

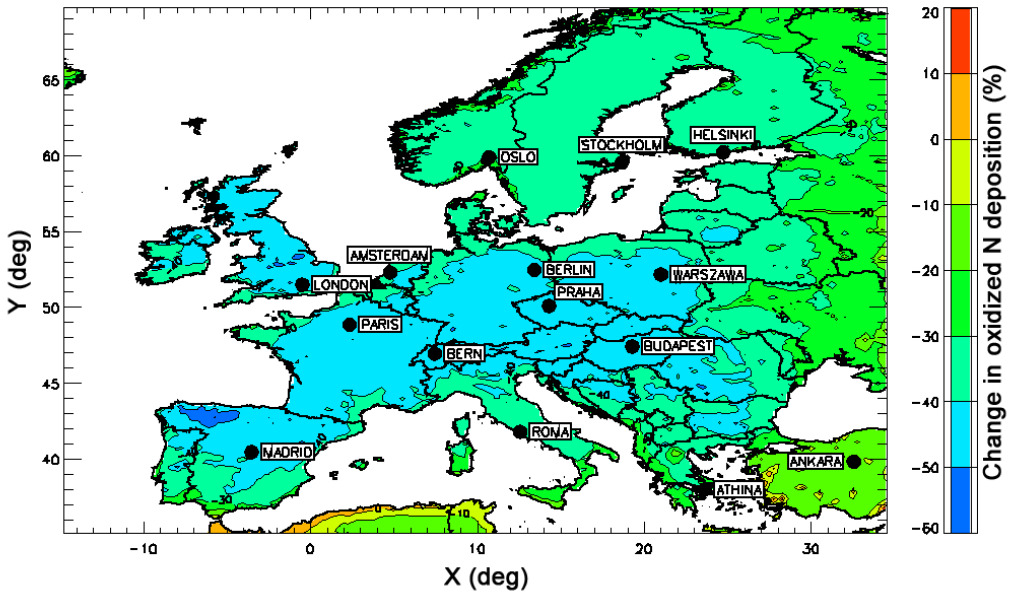

1

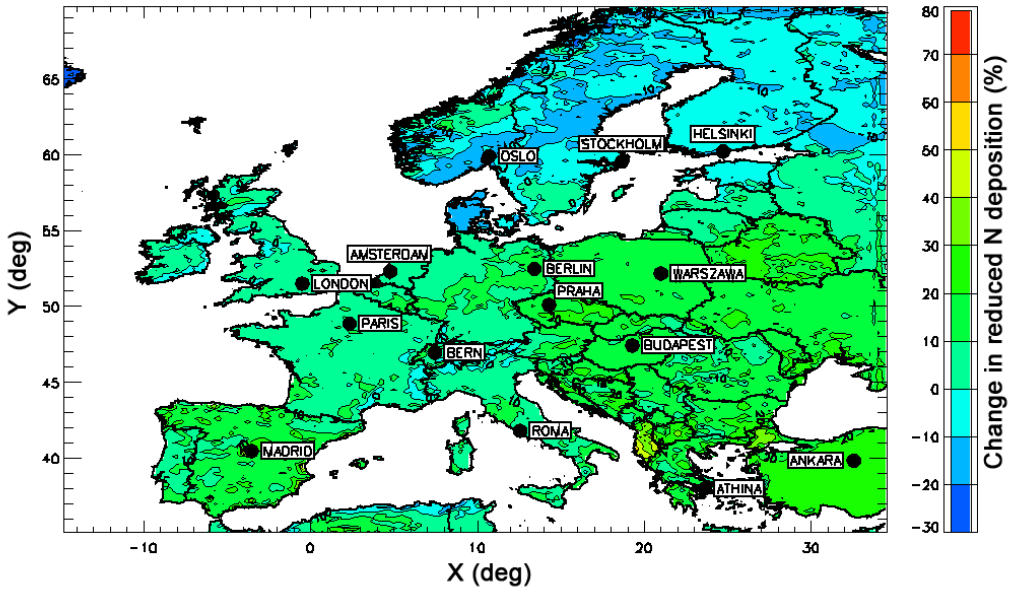

2

3 Figure 17: Relative changes in deposition of oxidized (upper panel) and reduced (lower
4 panel) nitrogen species over the European domain, BL 2020 – 2005.

5

6

7